Mineralium Deposita (2001) 36: 300–331
DOI 10.1007/s001260100178

ARTICLE

Raimundo NetunoVillas · Marcio Dias Santos

Gold deposits of the Carajás mineral province: deposit types and metallogenesis

Received: 7 May 2000 / Accepted: 12 March 2001 / Published online: 11 May 2001

Abstract The Carajás mineral province is located in the south-eastern part of the Amazon craton and is divided into the southern and northern tectonic blocks, which are referred to as the Rio Maria granitoid–greenstone terrane and the Itacaiúnas shear belt, respectively. The geological evolution of this province occurred almost entirely in the Archean, with no tectonism from ~2.4 to 1.9 Ga and then an episode of very extensive intraplate granitic magmatism. Distinct types of gold deposits, most associated with Archean metavolcano-sedimentary sequences, including greenstone belts as old as 2.9 Ga, comprise (1) Fe-oxide-poor Cu–Au, (2) Fe-oxide–Cu–Au–U–REE, (3) shear-zone related lode-gold, and (4) sedimentary rock-hosted Au–PGE. The shear-zone related deposits are more typical of the Rio Maria granitoid–greenstone terrane, whereas the other types are more abundant in the Itacaiunas shear belt. The first type, represented by the Serra Verde deposit, shows most characteristics of volcanogenic massive sulfide (VMS) deposits, except for the dominance of chalcopyrite over pyrite and/or pyrrhotite. Some deposits of the second type (Igarapé Salobo and Igarapé Bahia) are also syngenetic, but their ore mineralogy and paucity of pyrite and/or pyrrhotite are inconsistent with, or at least unusual for, classic VMS deposits. Other Fe-oxide–Cu–Au–U–REE deposits, such as the Cristalino and Sossego, occur as epigenetic stockwork mineralization related to Archean granitoid stocks. Most shear-zone related lode-gold deposits are classified as orogenic gold deposits (e.g. Sapucaia, Babaçu and Tucumã) that cut greenstone belt rocks. The Cumaru deposit is also hosted by a shear zone, but may have a genetic association with a granitoid intrusion. The Águas Claras deposit, although also hosted in a shear zone and perhaps intrusion-related, differs from the orogenic gold deposits by its extensional tectonic setting, lack of CO_2 in the ore fluids, and voluminous chalcopyrite. The sedimentary rock-hosted Serra Pelada Au–PGE deposit is structurally controlled and occurs in an Archean clastic-chemical sedimentary rock sequence.

R. NetunoVillas (✉)[1] · M.D. Santos (✉)[2]
Centro de Geociências,
Universidade Federal do Pará, Brasil
[1] E-mail: netuno@ufpa.br
[2] E-mail: mds@ufpa.br

Introduction

The Carajás gold province is part of the larger Carajás mineral province (CMP; Santos 1981), where significant reserves of iron, copper, gold, manganese and bauxite have been discovered. Practically unknown until the discovery of the iron ores in 1967, most of the knowledge of its geology has been collected during the last two decades. Docegeo, a subsidiary of the formerly government-owned Vale do Rio Doce Mining Company (CVRD), has undertaken much of the exploration in the region and its great mineral potential.

Gold has driven the majority of the exploration activity in the area, particularly after the boom of the Serra Pelada garimpo, attracting 40,000 gold-diggers in the early 1980s in the most spectacular gold rush ever seen in the Amazon jungle. A large number of different gold deposits have since been discovered, but only a few have been studied in detail. Moreover, important data have yet to be published, and are currently only available in theses and extended abstracts from local symposium volumes. This paper is an effort to synthesize these data from CMP. Its aim is to describe the main characteristics of the gold-bearing deposits in order to propose not only a preliminary classification, but also genetic models that can be useful for establishing exploration guidelines.

Tectonic setting

The CMP occurs in the Archean nucleus of the southern portion of the Amazon craton, known as the Central Brazil shield (Figs. 1 and 2). To the east, the province is cut by the N–S-trending, Neoproterozoic Araguaia fold belt (Moura and Gaudette 1993) whereas, to

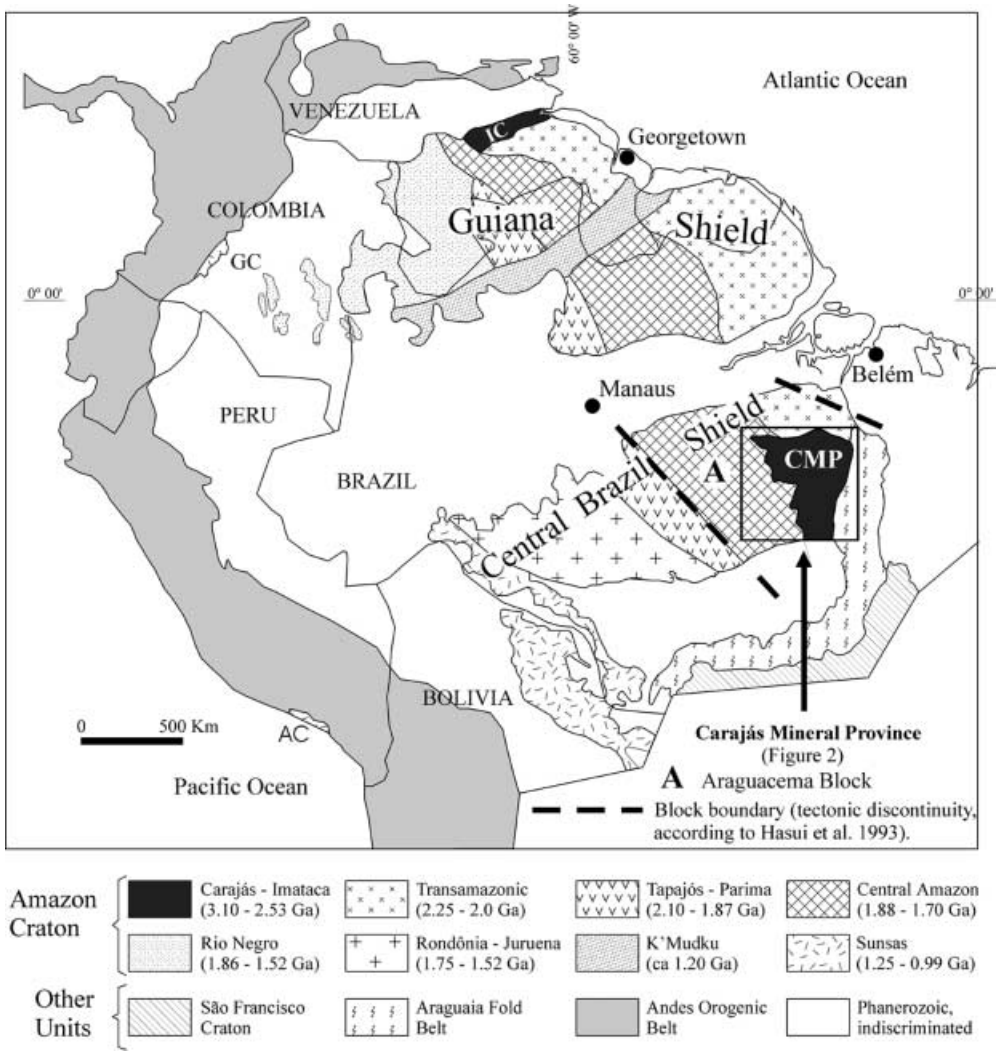

Fig. 1 Major geochronological provinces of the Amazon Craton in northern South America (modified from Santos et al. 2001). *GC* Garzon Complex, Grenvillean; *AC* Arequipa Complex, Grenvillean; *IC* Imataca Complex; *CMP* Carajás Mineral Province

the west, it is overlain by the Palaeoproterozoic volcano plutonic and sedimentary rocks of the Uatumã Supergroup (Cunha et al. 1981; Costi et al. 2000). The northern boundary is marked by the Transamazonic Province (or the Maroni-Itacaiunas mobile belt of Cordani et al. 1979) and in the south, limits are not well defined, although Inajá Ridge may be considered as the southern boundary.

Two early hypotheses differ about the Proterozoic tectonic evolution of the Amazon craton. One defines the craton as solely a large Archean platform, slightly reworked and reactivated during Proterozoic times (Amaral 1974, 1984; Almeida 1978; Schobbenhaus and Campos 1984; Hasui and Almeida 1985), and with the Carajás region being a subprovince of the Central Brazil shield. The other hypothesis holds that the post-Archean evolution of the Amazon craton was the result of successive Proterozoic terrane accretion episodes (Cordani et al. 1979, 1984; Cordani and Brito Neves 1982; Teixeira et al. 1989; Sato and Tassinari 1997; Tassinari and Macambira 1999). Despite these differences in interpretation, there is general agreement that the CMP is an Archean nucleus to the Amazon craton, which is represented by granitoid–greenstone terranes and high-grade metamorphic complexes, which were only slightly affected by Proterozoic tectonic events.

A third model for the Archean and Proterozoic evolution of the Amazon craton has combined robust radiometric ages with gravimetric and magnetometric data (Hasui et al. 1993). Such an approach led to the definition of a series of large crustal blocks bounded by major sutures. The nuclei of these blocks are typically represented by granitoid–greenstone terranes. This model implies a complex collisional history of northern Brazil prior to 1.8 Ga. According to this model, the CMP lies in the so-called Araguacema block.

More recently, Santos et al. (2001), based on U–Pb and Sm–Nd isotopic data, define the Carajás–Imataca province as the only Archean province of the Amazon craton. The neighbouring Palaeoproterozoic Central Amazon province (Fig. 1) truncates the Carajás tectonic trends and was generated by partial melting of Archean continental crust.

Regional geology

Lithostratigraphy

The boundary between the northern and southern crustal segments into which the CMP has been divided (Fig. 2) appears to be transitional. The southern segment is known as the Rio Maria granitoid–greenstone terrane (RMGGT; Huhn et al. 1988), and is older than the northern segment, referred to as the Itacaiunas shear belt (ISB; Araujo et al. 1988).

The oldest units that have been mapped in the RMGGT (Table 1) are the Late Archean Xingu Complex and the Andorinhas Supergroup (Docegeo 1988; Araújo et al. 1988; Faraco et al. 1996). The Xingu Complex (Silva et al. 1974) has long been considered to represent the basement rocks of the province, and it is made up of high-grade gneisses and migmatites, varying in composition from granodiorite to tonalite. Recently, the Arco Verde

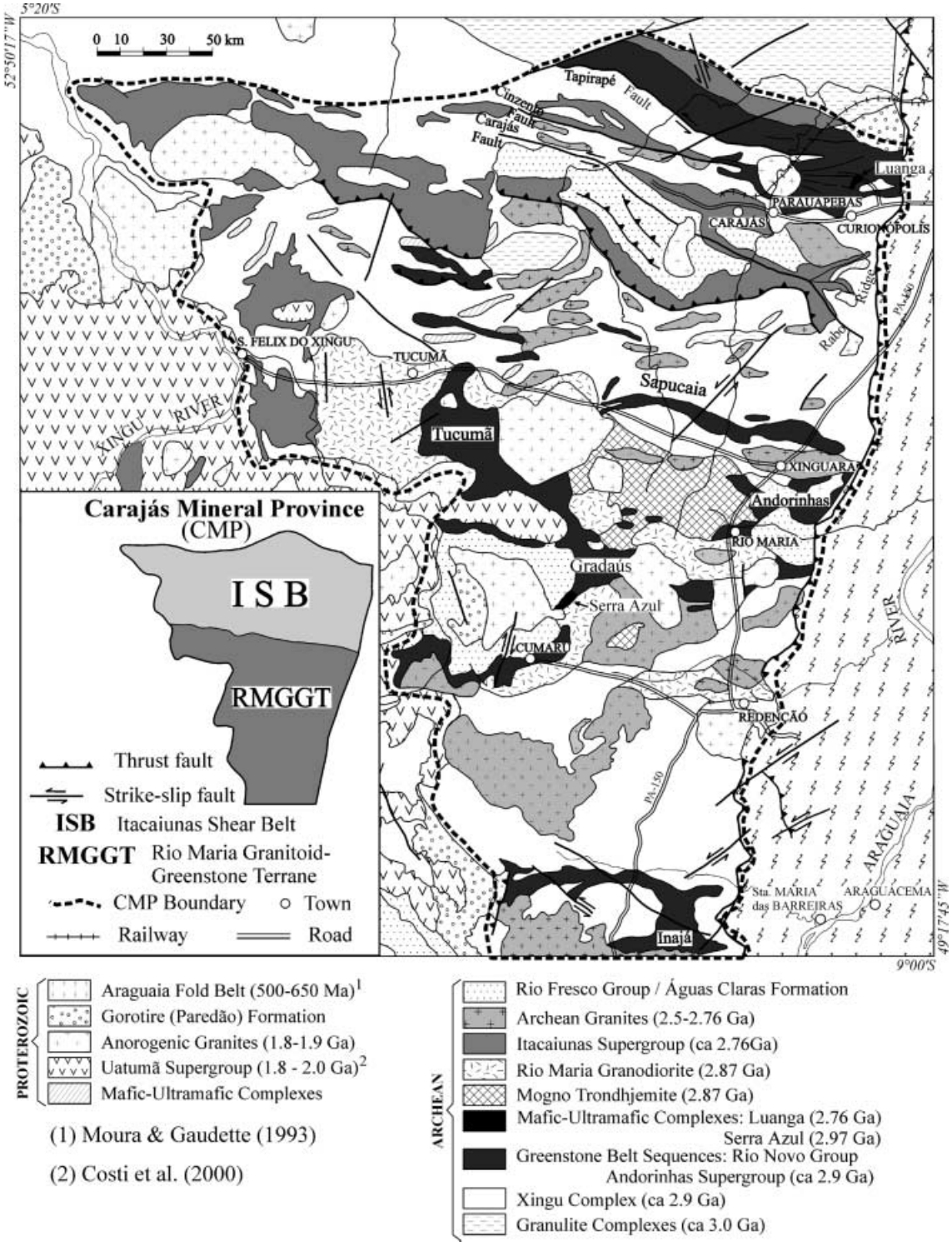

Fig. 2 Geological map of the Carajás Mineral Province (adapted from Schobbenhaus et al. 1981, Docegeo 1988 and Faraco et al. 1996). Age sources in Table 2, except for the Araguaia Fold Belt (*1*) and the Uatumã Supergroup (*2*)

tonalite was separated from the Xingu Complex as a distinct unit owing to its geological similarities with the Rio Maria granitoid–greenstone terrane and its TTG affiliation (Althoff et al. 1995).

The Andorinhas Supergroup is a greenstone sequence composed of ultramafic and mafic metavolcanic rocks, intercalated with iron formations at the base (Babaçu Group) and chemical and clastic metasedimentary rocks at the top (Lagoa Seca Group). Similar greenstone sequences, known as the Tucumã, Gradaus, and Sapucaia Groups, occur elsewhere. The Serra do Inajá Supergroup is a similar sequence defined for the Inajá greenstone belt (Docegeo 1988) in the southernmost portion of the CMP. Large Archean batholiths, referred to as the Rio Maria granodiorite, the Mogno trondhjemite and the Parazonia tonalite, cut the greenstone rocks. Deformed Archean calc-alkaline plutons, such as Mata Surrão, Cumaru and Xinguara, are clearly intrusive into the previous units. The Archean Serra Azul

Table 1 Stratigraphic column of the Carajás Mineral Province (modified from Docegeo 1988)

Eras	Ga	Rio Maria granitoid–greenstone terrane			Itacaiunas shear belt		
		Complexes or supergroups	Groups or formations	Intrusive rocks	Complexes or supergroups	Groups or formations	Intrusive rocks
Proterozoic	1.9			Anorogenic granites (Musa, Jamon, Bannach, Gradaús, Seringa, etc.)			Anorogenic granites (Serra dos Carajás, Cigano, Pojuca, Antônio Vicente, etc.)
							Santa Inês gabbro (?)
Archean	2.5						Old Salobo, Itacaiunas and Planalto granites
	2.6						Basic dikes and sills
			Rio Fresco Group			Águas Claras Formation	Plaquê granitoid suite
	2.8				Itacaiunas Supergroup	Buritirama, Igarapé Bahia, Grão Pará, Igarapé Pojuca, Igarapé Salobo Groups	Borrachudo mafic intrusion(?)
				Mata Surrão and Xinguara granites, Mogno trondhje mite, Rio Maria granodiorite, Parazonia tonalite		Rio Novo Group(?)	Luanga ultramafic intrusion, Estrela granite
			Tucumã, Sapucaia(?), Gradaús(?) Groups				
	2.9	Andorinhas and Serra do Inajá Supergroups	Lagoa Seca/ Babaçu and Rio Preto/ Santa Lúcia Groups	Arco Verde tonalite and Serra Azul ultramafic intrusion			
	3.1	Xingu Complex			Xingu and Pium Complexes		

mafic–ultramafic intrusion, which intrudes the Gradaus greenstone sequence, is also exposed in the Rio Maria region.

In the northern segment of the CMP, where the ISB is developed, the Late Archean basement is, in addition to the Xingu Complex, also interpreted to be comprised of rocks of the Pium Complex (Table 1), which corresponds to lower crustal granulitic rocks that have been thrust up along shear zones. A series of metavolcano–sedimentary sequences overlie the basement rocks. One of these, the Rio Novo Group, is a greenstone belt that is slightly younger than those of the RMGGT and contains significant Fe–Cu–Au mineralization. The others, known as the Igarapé Salobo, Igarapé Pojuca, Igarapé Bahia, Grão Pará and Buritirama Groups, are greenstone-like sequences collectively grouped in the Itacaiunas Supergroup. The first three host additional Fe–Cu–Au deposits, whereas the latter two enclose banded iron and manganese formations, respectively. Mafic magmatism is dominant, and all lithostratigraphic units appear coeval, despite different metamorphic grades and deformation intensities. Several elongated, E–W-trending Archean granitic bodies, known as the Plaquê Suite, intrude rocks of the Xingu Complex. Likewise, other Late Archean intrusions include the syntectonic, subalkaline Estrela granite (Barros 1997) and the Old Salobo granite (Lindenmayer 1990), which cut rocks of the Rio Novo and the Igarapé Salobo Groups, respectively. Probably contemporaneous with deposition of rocks of the Rio Novo Group was the emplacement of the PGE- and chromite-bearing Luanga mafic–ultramafic intrusion (Suita 1988; Diella et al. 1995).

An extensive Late Archean marine to fluvial, mostly clastic, succession covers large areas of the CMP. It is weakly metamorphosed and has been named the Rio Fresco Group (Cunha et al.1984) or Águas Claras Formation (Araújo et al. 1988; Nogueira et al. 1995), with the latter designation so far restricted to exposures in the Carajás basin.

The emplacement of many anorogenic alkaline to subalkaline granitic stocks and batholiths, some of which are mineralized with tin or tungsten, occurred in Palaeoproterozoic times. These intrusions show the chemical and tectonic characteristics of A-type granites (Dall'Agnol et al. 1994). From south (RRGGT) to north (ISB), important intrusions include the Gradaús, Redenção, Bannach, Musa, Jamon, São João, Seringa, Velho Guilherme, Serra dos Carajás and Cigano bodies (Figs. 4 and 8).

The province was also affected by a number of more local mafic magmatic events represented by (1) sills and dikes that cut rocks of the Águas Claras Formation, and possibly also the Igarapé Pojuca and Igarapé Bahia Groups; (2) the Fe- Ti- and P-rich Borrachudo gabbroic body; (3) the Santa Inês gabbro; and (4) the Lago Grande Complex gabbroic rocks. The former are Late Archean, and the latter three have not been dated.

Structural evolution

The RMGGT and the ISB can be differentiated in terms of both their geological setting and associated mineral deposits. According to Costa et al. (1995), the main structures of the Rio Maria granitoid–greenstone terrain are E–W, NW, and NE-trending shear zones. They represent dextral strike-slip faults that have affected

chiefly the supracrustal rocks. Synformal structures along the shear directions, previously interpreted as synclinoria (Silva et al. 1974), are considered to be transpressive duplexes (Araújo et al. 1988). The larger duplexes are related to E–W shear zones (Andorinhas and Gradaus), whose cores consist of sedimentary rocks of the Rio Fresco Group and whose borders are defined by thrust faults.

The Carajás Ridge (Fig. 2), in the ISB, was initially assumed to be a large synclinorium (Knup 1971; Beisiegel et al. 1973; Silva et al. 1974) and, later, a positive flower structure (Araújo et al. 1988). This flower structure is interpreted to have been developed in two stages: (1) an earlier dextral transtension event that accounted for pull-apart basins controlled by E–W trending strike-slip faults and (2) a subsequent sinistral transpression event that inverted the basins, giving rise to push-up structures such as transpressive duplexes.

A more recent interpretation (Pinheiro 1997; Pinheiro and Holdsworth 1997) maintains that the inversion caused only complex folding and sinistral strike-slip faulting. Based on the geochemical signature of the basaltic rocks and the primary structural features preserved in the sedimentary units, these authors also argued that the deposition of the volcano-sedimentary sequences of the Itacaiunas Supergroup was in large intracratonic, rather than in pull-apart basins, as had been earlier suggested (Gibbs et al. 1986; Wirth et al. 1986; Nogueira 1995; Nogueira et al. 1995). This new hypothesis envisages the tectonic evolution of the ISB in five stages: (1) sinistral transpression (2.9–2.85 Ga) with high-temperature ductile deformation affecting the basement rocks and those of the Igarapé Salobo Group; (2) sinistral transpression (2.8–2.7 Ga) with low-temperature ductile–brittle deformation affecting rocks of the Igarapé Pojuca Group; (3) formation of intracratonic basins ($<$2.76 Ga) leading to deposition of the Grão Pará Group and the Águas Claras Formation; (4) dextral transtension (2.7–2.6 Ga) with the development of the Carajás and Cinzento strike-slip fault systems in which the rock units are down-faulted inside major dilational jogs and cut by mafic sills and dikes; and (5) sinistral transpression ($<$2.6 Ga) with very low-temperature brittle to ductile deformation of the rocks immediately adjacent to the Carajás and Cinzento fault systems, together with weak tectonic inversion by fault reactivation.

At about 1.9–1.8 Ga, the whole CMP was affected by a regional extension event. This tectonism facilitated the intrusion of A-type granitic plutons and dike swarms.

Metamorphism

High-grade metamorphic rocks have only been mapped in the basement units. Most supracrustal rocks of both the Andorinhas and Itacaiúnas Supergroups have been subjected to greenschist- to amphibolite-facies conditions, with regional metamorphic temperatures seldom exceeding 700°C (Lindenmayer 1990). Earlier widespread hydrothermal submarine metamorphism affected the Itacaiunas volcano-sedimentary sequences prior to the regional metamorphic events, as can be deduced from the abundance of water-saturated minerals and relict textures in the mafic metavolcanic rocks. In fact, undeformed rocks, composed of variable amounts of decalcified plagioclase, epidote, chlorite, tremolite–actinolite, white mica, quartz and carbonates, are dominant in many units, particularly in rocks of the Grão Pará and Igarapé Bahia Groups.

Thermal aureoles associated with some granitic intrusions are commonly superimposed on the submarine and regional metamorphic assemblages. In a few cases, anthophyllite–cordierite rocks occur, as in the mafic metavolcanic rocks of the Igarapé Pojuca Group (Medeiros Neto and Villas 1985; Winter 1995). In others, as for example surrounding the Estrela granitic complex, pyroxene hornfels and albite–hornblende hornfels facies record temperatures in the 600–650 °C range near the intrusion contacts (Barros 1997).

Geochronology of the Carajás mineral province

A great deal of radiometric data are available for the rocks in the CMP (Table 2). Many are robust ages based on the U–Pb zircon method, including a few obtained by the SHRIMP technique. Many others are Pb–Pb ages on whole-rock or zircon, which provide values in very good agreement with the U–Pb dating. Some Rb–Sr results have been published but, as expected, the ages are systematically younger when compared with more robust methods.

Except for the Palaeoproterozoic granitoid magmatism and minor mafic to intermediate igneous events of unknown age, the rocks of the CMP are mainly Late Archean in age. Available geochronological data indicate most rocks formed from ~3.0 to 2.4 Ga. There was a ≈500-million-year-long hiatus in the formation of new crust, with then the onset of the widespread Palaeoproterozoic tectonism and magmatism at ~1.9–1.8 Ga (Fig. 3).

Excluding the metamorphism of the basement rocks at ~2.9–3.0 Ga, no age older than 2.76 Ga has been measured in the ISB supracrustal rocks and granitoids. The tectonically distinct RMGGT, appears to have been mainly formed ≈100 million years earlier than most of the ISB.

Nature of gold deposits

Types of gold deposits

In the CMP, primary gold mineralization occurs in four major types of deposits, which are defined by their mineral content, host rocks and controlling structures. Type I comprises Fe-oxide-poor Cu ± Au deposits hosted by Archean metavolcano-sedimentary rocks. Type II includes Fe-oxide–Cu–Au–U–REE deposits hosted by either Archean metavolcano-sedimentary rocks or granitoids. Despite the same metal suite, these do not appear to be Olympic Dam type deposits. Type III corresponds to shear-zone-related lode-gold deposits and type IV refers to sedimentary-rock hosted Au–PGE deposits, with the former being divided into the orogenic gold and copper–gold ± tungsten subtypes. Table 3 summarizes the most important features of the different Carajás gold deposits in terms of host rocks, metamorphism, tectonic setting, structural controls, ore and gangue mineralogy, wallrock alteration, associated metals and fluid composition. All deposit types are restricted to the ISB, except for type III orogenic gold deposits, which are concentrated in the Rio Maria region.

Type I (Fe-oxide-poor Cu ± Au deposits)

The Serra Verde deposit, near the city of Parauapebas (Fig. 4), is the only type I deposit so far identified in the CMP. It is a small deposit that has undergone only small-scale mining. Restricted to the gold-enriched supergene zone and a few resistant quartz veinlets, workings occur on two, 20- to 30-m-long, copper- and iron-rich massive sulfide lenses with gold contents of 0.5–1 g/t.

Rocks of the Rio Novo Group (Hirata et al. 1982; Araújo et al. 1988) host the auriferous iron- and copper-bearing sulfide mineralization (Fig. 5). Amphibolites, schists, metagreywackes and iron formations are the main lithological types; ultramafic rocks are less common. In the Serra Verde deposit itself, clastic metasedimentary rocks are more abundant and are frequently intercalated with tholeiitic metavolcanic rocks.

Table 2 Summary of some geochronological data available for the Carajás Province rocks. *ZR* Zircon; *TIT* titanite; *MAG* magnetite; *WR* whole rock

	Geological units	Ages (Ma)	Methods	Sources[a]
Proterozoic granites	Jamon granite	1,601 ± 42	Rb–Sr (WR)	20
	Seringa granite	1,730 ± 58	Rb–Sr (WR)	19
	Velho Guilherme granite	1,653 ± 14/1,873 ± 13	Rb–Sr (WR)/Pb–Pb (WR)	14/3
	Pojuca granite	1,874 + /–2	U–Pb (ZR)	1
	Musa granite	1,692 ± 22/1,883 + 5/–2	Rb–Sr (WR)/U–Pb (ZR)	13/1
	Serra dos Carajás granite	1,820 ± 49/1,880 ± 2	U–Pb (ZR)	8/1
	Cigano granite	1,731 ± 28/1,883 ± 2	Rb–Sr (WR)/U–Pb (ZR)	17/1
Archean granites	Xinguara granite	2,528 ± 21/~2,880	Rb–Sr (WR)/U–Pb (ZR)	23/6
	Mata Surrão granite	2,541 ± 74/2,872 ± 10	Rb–Sr (WR)/Pb–Pb (WR)	7/3
	Itacaiunas deformed granite	2,560 ± 37	Pb–Pb (ZR)	11
	Old Salobo granite	2,573 ± 2	U–Pb (ZR)	1
	Plaquê Suite	2,736 ± 24	Pb–Pb (ZR)	2
	Cristalino diorites	2,738 ± 6	Pb–Pb (ZR)	18
	Planalto granite	2,747 ± 2	Pb–Pb (ZR)	18
	Estrela granite	2,527 ± 34/2,763 ± 7	Rb–Sr (WR) / Pb–Pb (ZR)	12/24
Itacaiunas Supergroup	Águas Claras gabbroic sill	2,645 ± 12	Pb–Pb (ZR)	10
	Igarapé Pojuca Group	2,732 ± 3	U–Pb (ZR)	1
	Igarapé Bahia Group	2,577 ± 72/2,747 ± 2	Rb–Sr (WR)/Pb–Pb (ZR)	9/25
	Grão Pará Group	2,758 ± 39/2,759 ± 2/ 2,760 ± 11	U–Pb (ZR)/U–Pb (ZR)/ U–Pb SHRIMP	8/1/16
	Igarapé Salobo Group	2,761 ± 3/2,776 ± 240	U–Pb (ZR)/Pb–Pb (MAG)	1/21
Ultramafic Complex	Luanga Complex	2,763 ± 7	U–Pb (ZR)	1
	Serra Azul ultramafic intrusion	2,970 ± 7	U–Pb (ZR)	5
Archean TTG	Cumaru granodiorite	2,817 ± 4	Pb–Pb (ZR)	22
	Parazonia tonalite	2,858	Pb–Pb (TIT)	5
	Mogno trondhjemite	2,871	Pb–Pb (TIT)	5
	Rio Maria granodiorite	2,739 ± 23/2,852 ± 16/ 2,872 ± 10/2,874 + 9/–10/ 2,872 ± 5	Rb–Sr (WR)/Pb–Pb (ZR)/ Pb–Pb (WR)/U–Pb (ZR)/ U–Pb (ZR)	14/2/3/4/5
Andorinhas Supergroup	Tucumã Group	2,868 ± 8	Pb–Pb (ZR)	2
	Lagoa Seca Group	2,904 + 29/–22/2,979 ± 5	U–Pb (ZR)	4/5
Basement rocks	Arco Verde tonalite	2,957 + 25/–21	U–Pb (ZR)	4
	Xingu Complex	2,859 ± 2/2,974 ± 15/ 2,971 + 30/–28/2,798	U–Pb (ZR)/Pb–Pb (ZR)/ U–Pb (ZR)/Pb–Pb (TIT)	1/2/4/5
	Pium Complex	3,050 ± 57/3,002 ± 14	Pb–Pb (WR)/U–Pb SHRIMP	3/15

[a] *1* Machado et al. (1991); *2* Avelar et al. (1999); *3* Rodrigues et al. (1992); *4* Macambira and Lancelot (1996); *5* Pimentel and Machado (1994); *6* Macambira (1992); *7* Duarte et al. (1991); *8* Wirth et al. (1986); *9* Ferreira Filho (1985); *10* Dias et al. (1996); *11* Souza et al. (1996); *12* Barros et al. (1992); *13* Gastal et al. (1987); *14* Lafon et al. (1991); *15* Pidgeon and Macambira (1998); *16* Trendall et al. (1998); *17* Gonçalez et al. (1988); *18* Huhn et al. (1999a); *19* Lafon et al. (1988); *20* Dall'Agnol et al. (1984); *21* Mellito and Tassinari (1998); *22* Lafon and Scheller (1994); *23* Macambira et al. (1991); *24* Carlos Eduardo Barros (personal communication); *25* Moacir B. Macambira (personal communciation)

The sulfide lenses are concordant to subconcordant with the foliation (both S_0 and S_1) of the host rocks (Fig. 5). One is enclosed by quartz- and chlorite-rich metabasalts with no major differences in the alteration assemblages of the hanging wall and footwall, except for the occurrence of quartz pods with sulfide minerals ± apatite ± ilmenite along the latter. The other lens is hosted by biotite–muscovite–quartz–chlorite schists. It shows much higher contents of gangue minerals whose erratic distribution in the sulfide matrix lends a brecciated aspect to the rock. Tourmaline is, in general, associated with the quartz- and chlorite-bearing rocks, occurring as either disseminations in the metabasalts or tourmalinites represented by continuous, thin layers (a few millimetres to 1 cm thick) parallel to the bedding planes in the metasedimentary rocks. Its composition is dravitic with Mg/(Mg + Fe) ratios that vary from 0.6 to 0.8, the higher values being more characteristic of the metasedimentary rocks (Reis 2000). The margins of the lenses are sharply defined. Mineralogically, the massive lenses are composed of more than 70% sulfide minerals, with variable proportions of silicate, oxide and phosphate minerals. The sulfide minerals include chalcopyrite (85%), pyrrhotite (5%), pyrite (3%), cubanite (3%), molybdenite (2%) and sphalerite (1%). Quartz, magnesium–hornblende or actinolite, ilmenite and fluorapatite, in decreasing order of abundance, are the major gangue minerals, with lesser biotite and magnetite. Mackinawite, stannite and stilpnomelane are minor constituents. Gold occurs as microscopic free particles in chalcopyrite (Reis and Villas 1999; Reis 2000). Disseminated mineralization is present in the host rocks, but the sulfide minerals

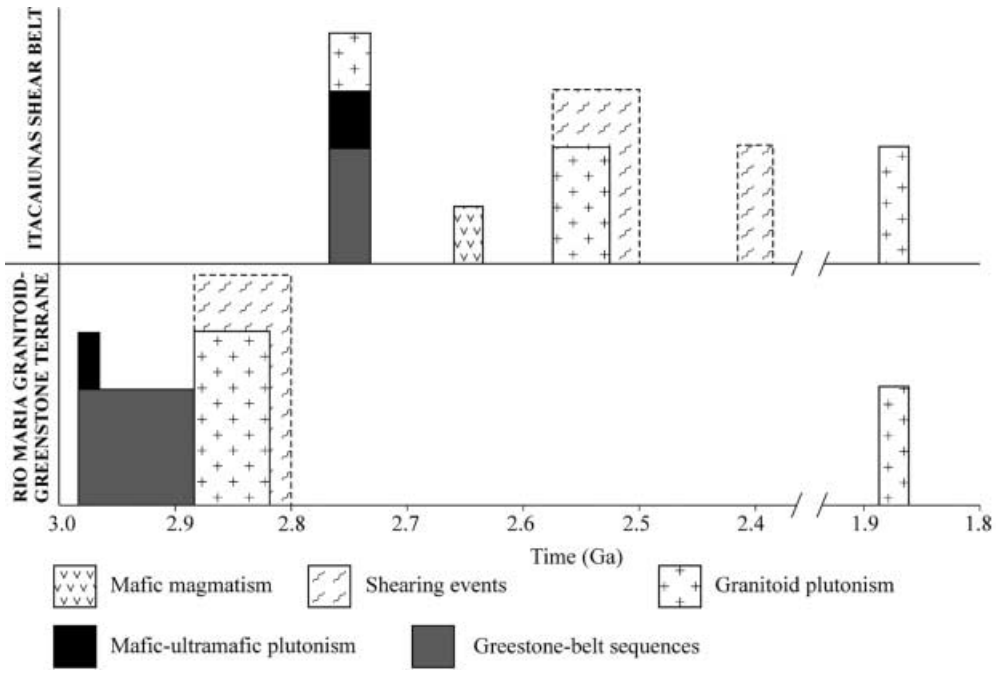

Fig. 3 Major geological events recorded in the Carajás Mineral Province from Archean to Paleoproterozoic times

represent less than 5% of the altered rock volume. Massive sulfide samples average 10 ppm Ag, 391 ppm Co, 1,479 ppm Ni and 545 ppm Zn. Total REE contents range from 2 to 65 ppm and uranium concentrations are below the detection limit (10 ppm) for the technique used (XRF on pressed powder samples).

Three distinct hydrothermal events have been identified at the Serra Verde deposit: (1) deposition of a volcano-sedimentary pile and associated circulation of heated seawater; (2) fluid flow during intrusion of the Estrela granitoid at 2,763 ± 7 Ma (Table 2); and (3) fluid circulation along fault planes during shearing (Reis 2000). Our observations favour deposition of ore minerals during the older sub-seafloor event.

Evidence for submarine hydrothermal activity comes chiefly from the widespread propylitization of the basalts of the Rio Novo Group, although they still partly preserve their original igneous textures. The quartz- and chlorite-altered rocks are most likely products of seawater–basalt interaction, consistent with well-documented observations on contemporaneous seafloor samples (Humphris and Thompson 1978) and experimental work (Mottl 1983). Similarly, dravitic tourmaline and its concentration in true tourmalinites are common features of seafloor exhalative activity (e.g. Slack 1996).

During the intrusion of the Estrela granitoid, primary mineral assemblages of the volcano-sedimentary pile were converted to hornblende–hornfels facies associations at 550–650 °C and within a ≈2-km-wide aureole (Barros 1997). In the sulfide lenses, granoblastic textures, polygonal grain contacts and porphyroblasts of the major gangue minerals, as well as pyrrhotite blasts and pyrite relicts, indicative of growth of pyrrhotite at the expense of pre-existing iron-rich sulfides, provide good evidence of this metamorphic overprinting. Several of these features are considered to be the result of recrystallization attaining an equilibrium fabric (Cook et al. 1993), whereas the transformation of pyrite to pyrrhotite certainly required temperatures well above 300°C (Craig and Vokes 1993).

These contact metamorphic features were overprinted by later hydrothermal alteration related to a sinistral NNE-trending brittle–ductile shearing event (Reis 2000). In addition to the formation of a 5-m-thick, sub-concordant barren quartz vein, rocks adjacent to the shear were altered to an assemblage of quartz, chlorite, actinolite, epidote, leucoxene and carbonates minerals. Although it is seldom easy to distinguish this assemblage from the older seafloor propylitic event, it can be defined as (1) the occurrence of vermicular chlorite replacing earlier secondary minerals, (2) the much higher degree of anhedralism of the quartz grains and (3) actinolite megacrystals (≤ 50 cm long), particularly developed in the quartz vein. In the sulfide lenses, microstructures such as kink bands, cubanite exsolution lamellae and ladder fractures in chalcopyrite, and duplexes filled with mackinawite and gold, are features that are interpreted to have been produced during the shearing event. Monoclinic pyrrhotite in some of these microstructures was also produced, implying temperatures in the range 200–270°C. Locally quartz veinlets with high gold grades occur, but it is uncertain whether they are related to the shearing.

Type II (Fe-oxide–Cu–Au–U–REE deposits)

Three deposits in the Carajás region may be included in the Fe-oxide–Cu–Au–U–REE type: Cristalino, Igarapé Salobo and Igarapé Bahia (Fig. 4). The former was recently discovered, so that much of the geological information is still preliminary (Huhn et al. 1999b, 2000). In

Table 3 Main geological characteristics of the Carajás gold deposits. *Ab* Albite; *Alm* almandine; *Ap* apatite; *Arspy* arsenopyrie; *Bn* bornite; *Bt* biotite; *Ca-amph* Ca-amphibole; *Calc* calcite; *Carb* carbonates; *Cc* chalcocite; *Cpy* chalcopyrite; *Cv* covelite; *Fa* fayalite; *Ferb* ferberite; *Fl* fluorite; *Grun* grunerite; *Hbl* hornblende; *Hem* hematite; *Ilm* ilmenite; *Kaol* kaolinite; *KF* potassic feldspar; *Mag* magnetite; *Po* pyrrhotite; *Px* pyroxene; *Py* pyrite; *Qz* quartz; *Scap* scapolite; *Ser* sericite; *Sid* siderite; *Stilp* stilpnomelane; *Tour* tourmaline

Deposit type	Host rocks	Metamorphism	Tectonic setting	Structural control	Wallrock alteration	Ore mineralogy	Gangue minerals	Hydrothermal fluids	Estimated resources
Fe-oxide-poor Cu–Au									
Serra Verde	Amphibolites, schists, metagreywackes	Thermal (hbl – hornfels); dynamic	Rift-type extensional basin	Superimposed shear zones	Silicification, propylitization, tourmalinization	Cpy, Po, Py, Mo, Au, Zn, Ni, Sn	Ilm, Ap, Qz, Ca-amph, Tour, Bt, Mag		Not available
Fe-oxide–Cu–Au–U–REE									
Cristalino	Intermediate to felsic volcanic rocks, iron-formations, diorites	Greenschist to Ab–Ep–amphibolite facies		Tectonic breccias	K-, Na- and Fe-metasomatism; silicification, chloritization, carbonatization	Cpy, Py, Au, REE, U, Co, Ni	Mag, KF, Bt, Ab, Scap, Carb, Chl, Qz		200 Mt Cu ores; 1.6% Cu; 0.25 g/t Au[a]
Igarapé Salobo	Iron-formations	px- to hbl-hornfels	Rift-type extensional basin	Superimposed shear zones	Chloritization, silicification, K-metasomatism	Bn, Cc, Cpy, Cv, Au, Fl, REE, U, Mo, Co, Ag	Mag, Grun, Fa, Alm, Qz, Bt	Aqueous saline and carbonic	Bodies B and C: 157 Mt Au ore 0.57 g/t Au[b]
Igarapé Bahia	Breccias of the Igarapé Bahia Group	Greenschist facies	Rift-type extensional basin		Chloritization, carbonatization, tourmalinization, silicification, biotitization	Cpy, Au, REE-minerals, uraninite, Fl	Fe–Chl, Sid, Mag, Stilp, Tour	Aqueous saline and carbonic	Alemão body: 170 Mt ore 1.5% Cu; 0.8 g/t Au[c]
Shear-zone related									
Orogenic gold									
Sapucaia	Greenstone belt sequences	Greenschist facies	Crustal block collision	D-Riedel faults and tension fractures	Propylitization and phyllic alteration	Au	Qz, Py, Tour		Not available
Cumaru	Greenstone belt sequences	Greenschist facies	Crustal block collision	Tension fractures and stockworking	Silicification, sericitization	Au, Py, Mo, Bi	Qz, Ser, Chl, Ep, Ab, Calc, Mag, Hem	Aqueous saline and carbonic	17 t Au ore, 10 g/t[d]
Cu–Au									
Águas Claras	Metarenites, metagabbros	Very low grade	Oblique tectonics	Brittle to brittle–ductile shear zones	Chloritization, sericitization, silicification, kaolinization, propylitization	Cpy, Arspy, Py, Au, Ferb, Ag, W, Sn	Qz, Chl, Mag, Hem	Aqueous saline	9.55 Mt ore, 2.43 g/t Au[e]
Sediment-hosted Au–PGE									
Serra Pelada	Metasiltstones, dolomitic marble, metasandstones	Very low grade contact metamorphism	Oblique tectonics	Folds, faults	Silicification, chloritization, propylitization, sericitization	Au, Pd-minerals, Pt, Co, Ni, Cu, Ag	Amorphous carbon, Qz, Ser, Hem, Kaol, Mn-oxides		30 t Au[f]

[a] Huhn et al. (1999b)
[b] Vieira et al. (1988)
[c] Barreira et al. (1999)
[d] Faraco et al. (1996)
[e] CA Medeiros Filho (personal communication 1996)
[f] Viveiros (1999)

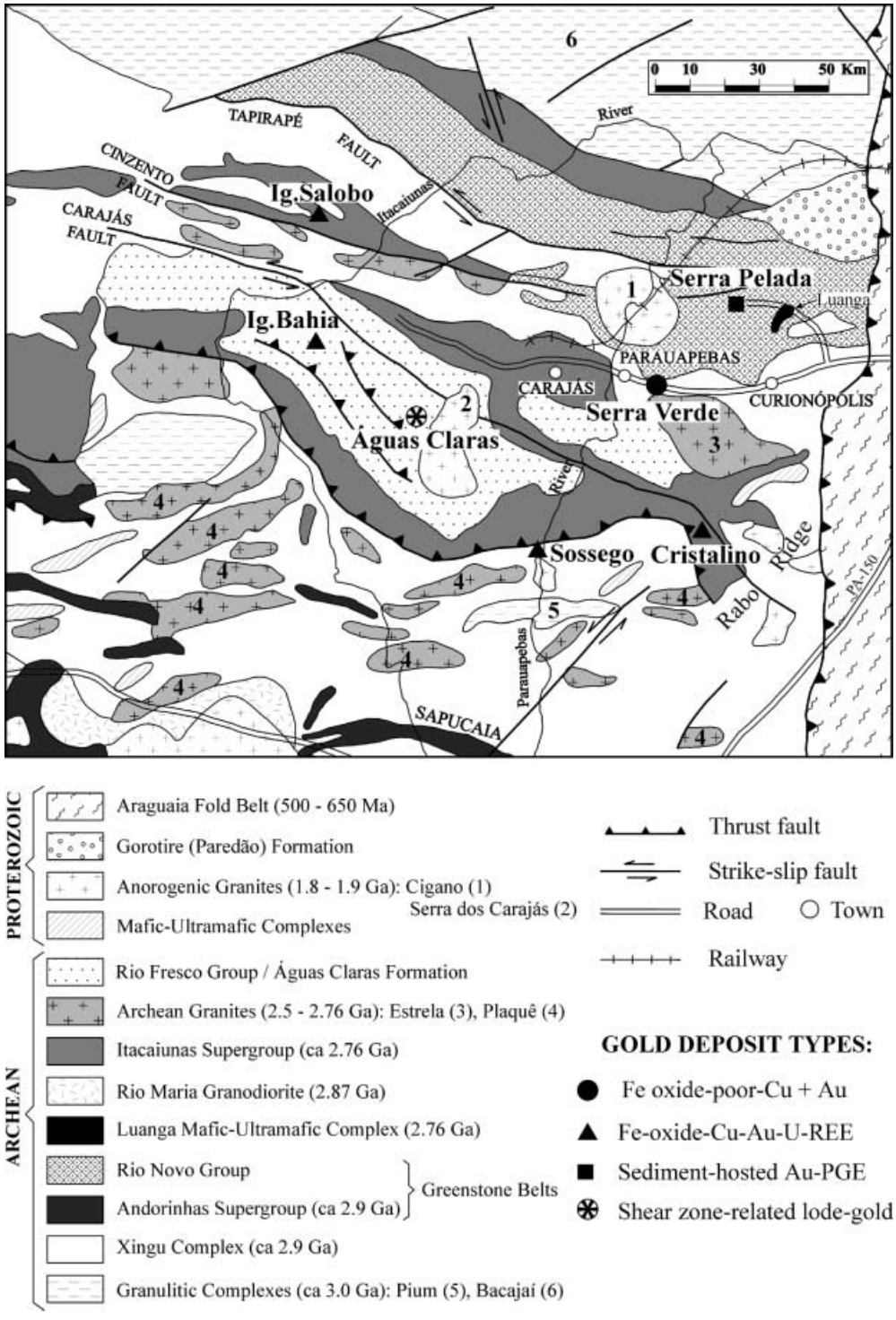

Fig. 4 Gold deposits of the Itacaiunas shear belt (adapted from Schobbenhaus et al. 1981, Docegeo 1988 and Faraco et al. 1996)

contrast, there is a large data base on the other two deposits, yet the data are ambiguous. The Sossego deposit (Fig. 4) can also be placed into this deposit type, but available data are only from the supergene environment from which the primary mineralization is inferred to consist of chalcopyrite, magnetite, subordinate pyrite and REE-bearing minerals (Huhn and Nascimento 1997). The Igarapé Salobo, Igarapé Bahia, Cristalino and Sossego deposits are hosted by metavolcanosedimentary sequences, but the associated intrusive rocks are only mineralized in the latter two (Huhn et al. 2000; Lancaster Oliveira et al. 2000).

Cristalino deposit

Located in the Rabo ridge area (Fig. 4), the Cristalino deposit is hosted by a low- to medium-grade

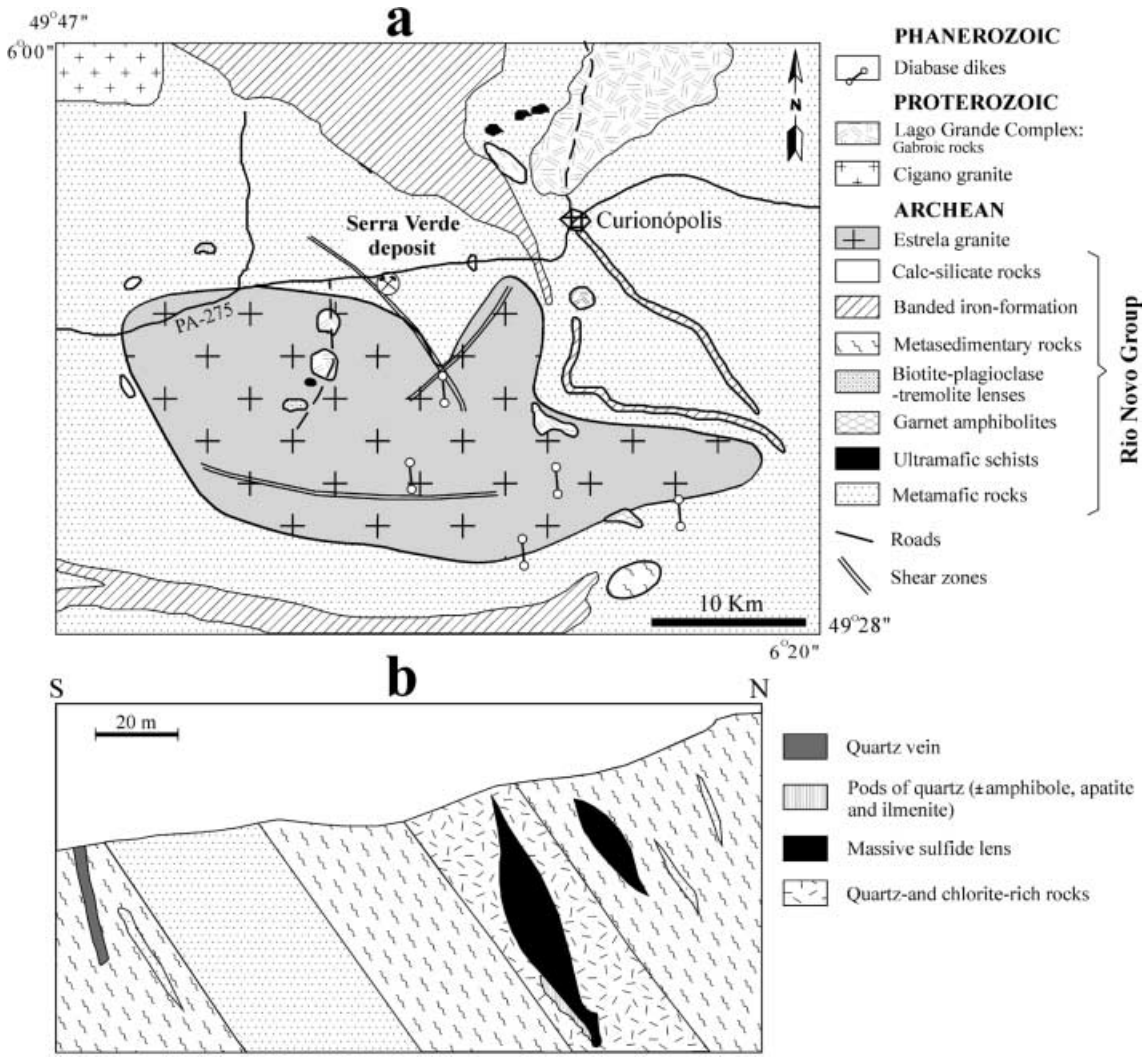

Fig. 5 **a** Geological map of the Curionópolis area and **b** schematic N–S cross section of the Serra Verde ore deposit (modified from Reis 2000)

metamorphic volcano-sedimentary sequence (Grão Pará Group?) in which intermediate to felsic volcanic rocks are intercalated with iron formations (Huhn et al. 1999b). Diorite and quartz diorite bodies (not shown in Fig. 4) have intruded this sequence, and are spatially and possibly genetically related to the mineralization. In addition to being strongly brecciated, the host rocks are hydrothermally altered to assemblages consisting of biotite, microcline, albite, scapolite, chlorite, carbonate minerals and quartz. They also show enrichment of phosphorus and iron metasomatism. White mica, zeolites and tourmaline are minor constituents, although locally they may be common. Allanite is believed to be the main REE source, but has been recorded only as an accessory phase in the host rocks.

The mineralization occurs in breccias and as stockworks, disseminations, and fracture fillings, in both the intrusive and metamorphic host rocks (Huhn et al. 1999b). Chalcopyrite, pyrite, magnetite, bravoite, cobaltite, millerite, vaesite and gold are the main ore minerals. One drill core revealed a 40-m-thick mineralized zone averaging 1.6% Cu and 0.25 g/t Au. The resource is estimated at greater than 500 Mt with grades of 1.0% Cu and 0.3 g/t Au (Huhn et al. 2000).

Igarapé Salobo deposit

The Igarapé Salobo deposit comprises four orebodies, termed A, B, C and D (Fig. 6). It is hosted by rocks of the 300- to 600-m-thick Igarapé Salobo Group, which is made up of metagreywackes intercalated with iron formations and minor amphibolites and arkosic quartzites. The amphibolites occur in the lower part of the sequence, near the contact with the basement rocks, whereas the iron formations are mostly in the lower part of the upper half, decreasing in abundance towards the top of the sequence. These iron formations occur as continuous to discontinuous, massive to foliated bands or lenses with thicknesses that vary on a centimetre to metre scale. They show gradational contacts with the enclosing metagreywackes (Lindenmayer and Teixeira

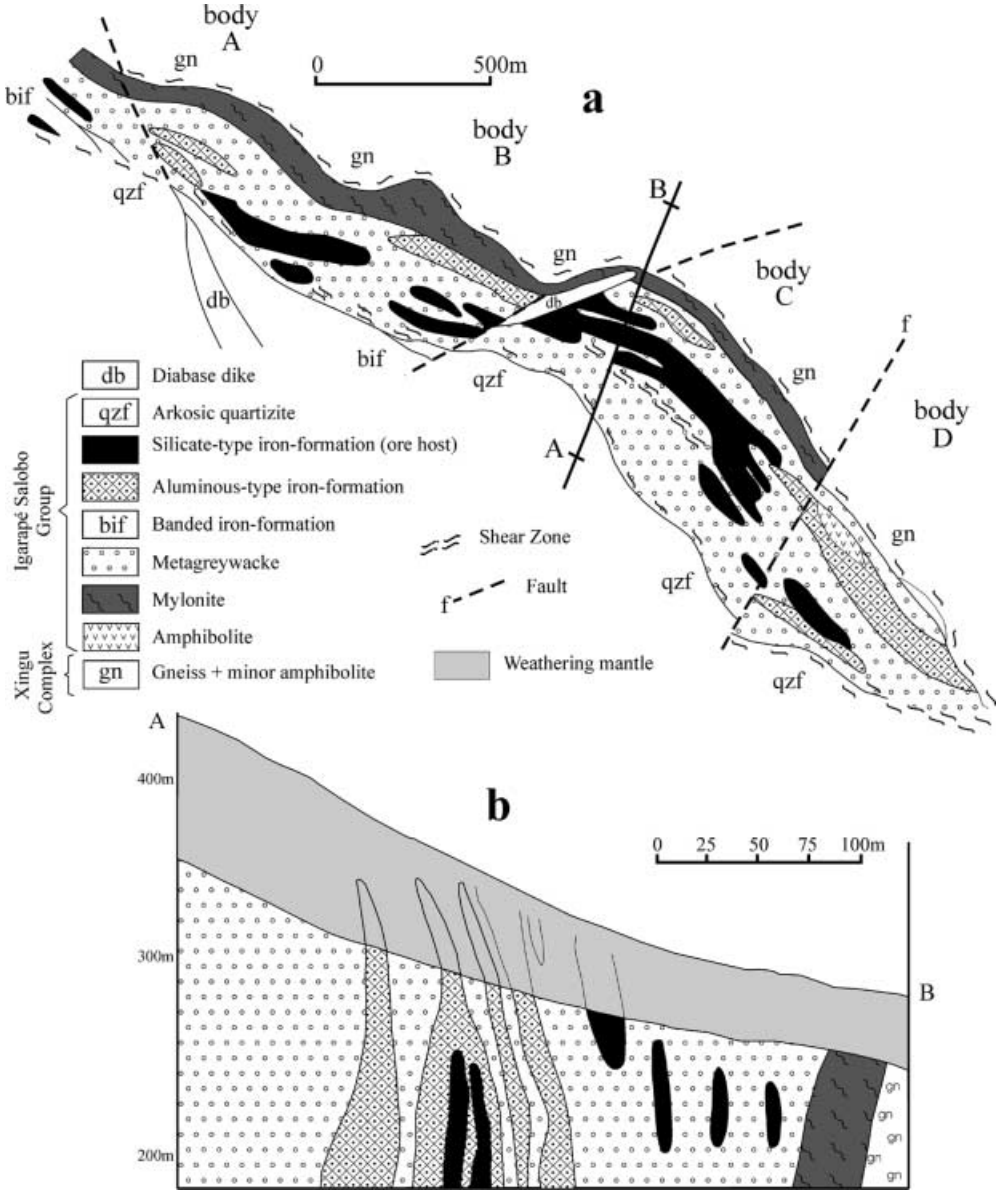

Fig. 6 **a** Geological map and **b** cross section of the Igarapé Salobo deposit at 250 m level (adapted from Vieira et al. 1988 and Lindenmayer 1990)

1999), and are concordant to subconcordant with the general trend of the Igarapé Salobo Group rocks. The term iron formation is used here in Trendall's sense (1983), referring to chemical sedimentary rocks with anomalously high iron contents. Two types of iron formation have been identified in the Salobo deposit (Lindenmayer and Teixeira 1999): (1) a silicate-type composed of magnetite, fayalite, grunerite, and minor hastingsite, Fe-biotite and Mn-almandine; and (2) an aluminous-type consisting of almandine, Fe-biotite, grunerite, magnetite and minor quartz.

The Igarapé Salobo rocks have been subjected to both an amphibolite facies metamorphic event and a shearing event dated, respectively, at 2,761 ± 3 and 2,555 + 4/–3 Ma (Machado et al. 1991). Shear zones trending N70–80°NW produced mylonitic-textured rocks with a schistosity that dips steeply to the south-west. Unexposed intrusive rocks are represented by the 2,573 ± 2 Ma Old Salobo granite (Table 2) and by a porphyritic quartz syenite (the so-called Young Salobo granite) with an Rb–Sr age of 1,880 ± 80 (Cordani 1981, in Lindenmayer and Teixeira 1999). At depth, the Old Salobo granite lies about 500 m south of the main mineralized zone, which is, in turn, clearly truncated by the Young Salobo granite.

Rocks of the Igarapé Salobo Group were locally metamorphosed to the pyroxene–hornfels facies (2–3 kbar; 750°C) and later hydrothermally altered to mineral associations compatible with the amphibolite (2.5 kbar; 650–550°C) and greenschist (< 370°C) facies (Lindenmayer 1990; Lindemayer and Teixeira 1999). The higher-temperature association involved a system dominated by magmatic fluids with f_{O2} equivalent to the QMF buffer and probably related to intrusion of the Old Salobo granite (Réquia et al. 1995). Potassic alteration of the high P–T facies was characterized by the assem-

blage chalcocite + Fe-biotite ± fayalite ± chalcopyrite ± hastingsite with tourmaline, allanite and zircon as accessory phases. During this hydrothermal activity, the contact metamorphosed rocks were enriched in Fe, K, Th, U and REE and depleted in Ca and Sr. Total REE contents are as great as 154 ppm in amphibolites and as much as 2,000 ppm in the iron formations. The lower-temperature associations probably resulted from the emplacement of the Young Salobo granite and consist of chlorite + epidote + albite + calcite + sericite + quartz (propylitic alteration), with greenalite + fluorite + uraninite.

Hypogene mineralization, which consists of disseminated to massive sulfides, occurs mainly in the silicate-type iron formations, with the higher copper and gold contents correlating with the increased magnetite abundances. Metagreywackes are essentially barren. Bornite, chalcocite and chalcopyrite, in order of abundance, are the chief sulfide minerals and are associated with minor amounts of ilmenite, molybdenite, covellite, graphite, uraninite, safflorite and cobaltite. Pentlandite, pyrrhotite and pyrite are rare. Chalcopyrite is more abundant in the fayalite-rich iron formations and is the main copper sulfide in late mineralized veins (Lindenmayer and Teixeira 1999). Bornite and chalcocite are preferentially concentrated in iron formations with magnetite >50% (Amaral et al. 1988). In addition, bornite and chalcocite contents are higher in grunerite-rich and quartz–chlorite-rich iron formations, respectively (Réquia et al. 1995) . According to these authors, magnetite grains present two major modes of occurrence: (1) idioblastic to subidioblastic crystals that show polygonal contacts with sulfides, but reactive borders with silicates, and formed via metamorphic recrystallization; minute grains of ilmenite, molybdenite, fluorite, apatite and uraninite are occluded in these crystals; and (2) lamellar grains produced by the breakdown of fayalite during subsequent hydrothermal events. No significant chemical differences exist between these two kinds of magnetite. Bornite and chalcocite occur as xenoblastic to subidioblastic grains or as myrmekitic intergrowths, the latter attributed to exsolution at low temperatures. Chalcopyrite is present in the intergranular spaces of fayalite, grunerite and magnetite, or as exsolution lamellae in bornite. According to Grguric and Putnis (1998), these lamellae are exsolved when bornite is subjected to high temperature. Evidence of metamorphism and deformation of sulfide grains is provided by microtextures related to mechanical flow and recrystallization (Siqueira and Costa 1991; Réquia et al. 1995).

Gold is principally present as submicroscopic (<0.1 μm) to microscopic (5–12 μm) particles in magnetite, chalcopyrite, cobaltite and safflorite grains, but it also occurs in the intergranular spaces between magnetite and chalcopyrite (Silva 1996b). Sporadically, it appears in undeformed quartz–calcite and copper–sulfides–chlorite–stilpnomelane veinlets that cut the iron formations. Microprobe analyses of free gold indicate concentrations of 6.98 to 10.82 wt% Cu, and subordinate amounts of Ag, Fe and As, implying precipitation at temperatures below 400°C (Chang et al. 1977; Réquia et al. 1995).

The average gold tenor of orebody C is 0.57 g/t, although higher values (0.8 to 4.5 g/t) occur locally in the iron formations, particularly those richer in magnetite (50–90%). Most gold is in magnetite grains, but microprobe bulk analyses on these grains failed to provide consistent concentrations for this precious metal (Silva 1996b). The more important orebodies B and C have a calculated reserve of 157 Mt at 0.57 g/t Au, with an additional 485 Mt at 0.19 g/t Au in the other two bodies (Vieira et al. 1988).

Fluid inclusion data from hydrothermal quartz and almandine crystals in the orebodies reveal carbonic ($CO_2 >> CH_4$) and variably-saline aqueous fluids (1.7 to >23.3 wt% equiv. NaCl), which have been suggested as metamorphic and magmatic in origin, respectively (Réquia et al. 1995).

Weathering processes have developed a ±50-m-thick supergene mantle, which includes a zone of secondary copper–gold mineralization, especially above the more sulfide-rich iron formations. Gold concentrations are erratic in the supergene zone, with contents in the range of 0.4–11.4 ppm (Silva 1996b).

Igarapé Bahia deposit

The Igarapé Bahia deposit, with extensive debate about its genesis, is the only large gold deposit presently being mined in the Carajás region. To date, all ore that feeds the Igarapé Bahia mill comes from the enriched supergene zone.

Geology of the deposit

In the deposit area, hydrothermally-altered metavolcano-sedimentary rocks of the Igarapé Bahia Group occur as a small erosional window within the overlying Águas Claras Formation (Fig. 4). The lower part of the group consists dominantly of mafic metavolcanic rocks intercalated with banded iron formations, whereas the upper part is made up of metasedimentary clastic rocks (metarhythmites, metasiltstones, metagreywackes) interbedded with intermediate to felsic metapyroclastic rocks, as well as with cherts and banded iron formations. Intercalations of metabasalts are subordinate in the upper part.

Separating these two parts of the Igarapé Bahia Group is an approximately 100-m-thick layer of hydrothermally-altered breccias, which in places show gradational contacts with the country rocks. Lithoclasts of mafic metavolcanic rocks, chert and banded iron-formation are dominant. These clasts, especially those of metavolcanic rocks, tend to be oriented parallel to the breccia contacts. Major constituents of the matrix are

chlorite, magnetite, carbonate minerals (siderite > ankerite) and chalcopyrite in different proportions, as well as minor amounts of quartz, tourmaline, biotite, grunerite-cummingtonite (more common in the Alemão orebody) and apatite. The clast/matrix ratio is highly variable, with clast-supported to matrix-supported breccias being present. These breccias may be products of phreatic hydrothermal activity (Almada 1998) in an environment where the influx of terrigenous sediments was common. Accordingly, they were formed prior to the tectonic movements that rotated the sequence subvertically (Fig. 7). The strongest evidence for a syn-sedimentary origin of the breccias is their almost invariable occurrence along the contact between the lower and upper parts of the Igarapé Bahia Group.

Rocks of the Águas Claras Formation lie unconformably over those of the Igarapé Bahia Group. They represent a thick sequence of slightly metamorphosed siliciclastic rocks in which the dominant metasandstones are interlayered with conglomerates and, less commonly, pelitic beds.

Later fracturing and faulting affected rocks of both the Igarapé Bahia Group and the Águas Claras Formation. This deformation was coeval with the intrusion of abundant gabbroic and dioritic dikes (Fig. 7). Calcite-rich veinlets also formed in the brittle episode.

Mineralization

The Igarapé Bahia deposit comprises four orebodies: Acampamento Norte, Acampamento Sul, Furo Trinta and Alemão (Fig. 7). The Alemão body, the most recent discovery (Barreira et al. 1999), is the only one that does not outcrop, being drill-intersected at a depth of about 250 m under the Águas Claras metasandstones (Soares et al. 1999). This orebody contains massive sulfide ore that is rare in the other three bodies. Ore reserves have not been published, except for the Alemão body, where 170 Mt have been measured with average grades of 1.5% Cu and 0.8 g/t Au (Barreira et al. 1999). Most of the mineralization occurs as disseminations in the hydrothermally altered breccias. In the Alemão orebody, massive sulfide lenses as thick as 40 m are noteworthy (Barreira et al. 1999). Sulfide disseminations also occur in the mafic metavolcanic rocks, whereas fine stratiform lenticules or nodules of sulfide minerals are more common in the pelitic rocks, particularly in the metarhythmites (Ferreira Filho 1985; Althoff et al. 1994; Lindenmayer and Bocalon 1997; Almada 1998). Another mineralization style includes veins and veinlets composed of quartz, chlorite, chalcopyrite, calcite and pyrite, with minor amounts of epidote, hematite, white mica, magnetite or titanite (Althoff et al. 1994).

Chalcopyrite is the most abundant sulfide mineral, no matter how rich the breccias are in magnetite or chlorite. Bornite is minor, although there are high contents in the Alemão orebody (Soares et al. 1999). A strong iron enrichment accompanied sulfide mineral deposition and accounted for the abundance of magnetite and/or iron-rich chlorite within altered breccia. Locally, concentrations of massive magnetite appear to have replaced the breccia. Massive fine- to medium-grained aggregates of siderite also replaced original minerals in the breccia. Among other sulfide minerals, pyrite and molybdenite are most common, but covellite and chalcocite are also present. Fluorite, REE-bearing carbonates, monazite, ferberite, hessite, uraninite, stilpnomelane, native gold and native silver occur as trace minerals (Sutec/CVRD 1996; Soares et al. 1999). Textural relations show that many minerals precipitated simultaneously, although a few were restricted to an early or late stage.

Chloritization, magnetitization, sulfidation and carbonatization were the main processes responsible for the hydrothermal alteration of the breccias, although minor silicification and tourmalinization also played a role. Biotitization is not common, but is developed locally in the Alemão orebody, whereas sericitization and albitization are rare throughout the whole deposit (Almada and Villas 1999; Soares et al. 1999).

Fluid inclusion studies of quartz from mineralized breccia (Almada 1998) reveal both aqueous and carbonic solutions. Two aqueous $NaCl–CaCl_2–(FeCl_2)$-bearing fluids have been identified. Fluids with lower salinities (5–23 wt% NaCl equiv.) and homogenization temperatures (110–140°C) are interpreted as modified seawater, whereas those that are more saline (28–36 wt% NaCl equiv.) and hotter (150–225°C) are considered to be derived from a magmatic source. The higher temperature field overlaps temperatures of 200–270°C obtained by chlorite geothermometry from both altered rocks and ores (Zang and Fyfe 1995). Raman spectroscopy data indicate that the carbonic fluids are pure CO_2 with traces of N_2. These fluids probably accounted for the abundant siderite and other carbonate minerals in the breccias. As chalcopyrite and magnetite, at least in part, precede siderite in the paragenetic sequence (Almada and Villas 1999), the earlier aqueous fluids are believed to have transported the copper and gold, although it is difficult to assess the role played by seawater versus magmatic water. Measured $\delta^{13}C_{PDB}$ values between –9.3 and $-5.8‰$ (Oliveira et al. 1998) are suggestive of a mantle source for the latter carbonic fluid.

Metal contents and ore reserves

Gold is intimately associated with the sulfide minerals, mostly as submicroscopic to microscopic free particles in chalcopyrite and to a lesser extent in pyrite (Lindenmayer and Bocalon 1997). It is also associated with monazite in the breccia matrix (Sutec/CVRD 1996). In the primary ore, gold contents as high as 1 g/t are common. Total REE concentrations are generally $< 0.7\%$ (Tallarico et al. 1998). The carbonate-rich breccias show ΣREE varying from 46.3–376.8 ppm with ΣLREE/ΣHREE ratios in the range of 8.5 to 17 (Lindenmayer and Bocalon 1997). Uranium contents vary

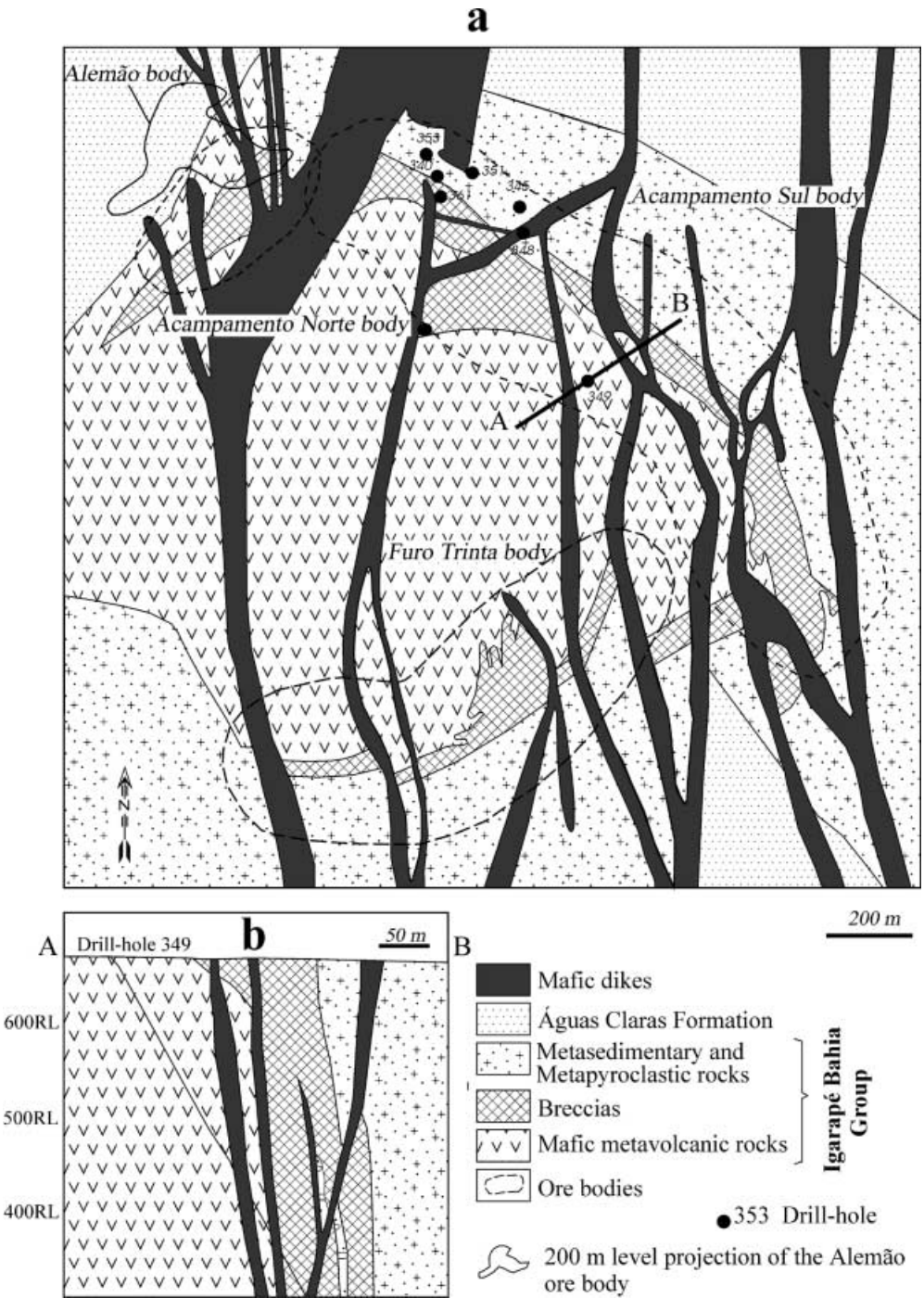

Fig. 7 **a** Geological map and **b** cross section of the Igarapé Bahia ore deposit (modified from Soares et al. 1999)

from 97–110 ppm in altered mafic volcanic rocks and from 14 to 160 ppm in magnetite-rich and siderite-rich breccias.

Type III (shear-zone-related lode-gold deposits)

Two subtypes of gold deposits have been identified within the shear zones in the CMP: orogenic gold and copper–gold ± tungsten deposits. Ubiquitous in Precambrian cratons, orogenic gold deposits, as defined by Roberts (1987), Groves and Foster (1991), Groves (1993), and Groves et al. (1998), are common in rocks of the RMGGT (Fig. 8). Examples include the Babaçu, Lagoa Seca, Cumaru, Sapucaia, Tucumã and Inajá deposits. These base metal-poor gold deposits generally occur in structurally-controlled quartz veins, with a few forming 200- to 500-m-long linear orebodies within the greenstone belt. The Lagoa Seca deposit is associated with neither quartz veins nor mafic metavolcanic rocks, and are hosted by magnetite-rich metagreywackes of

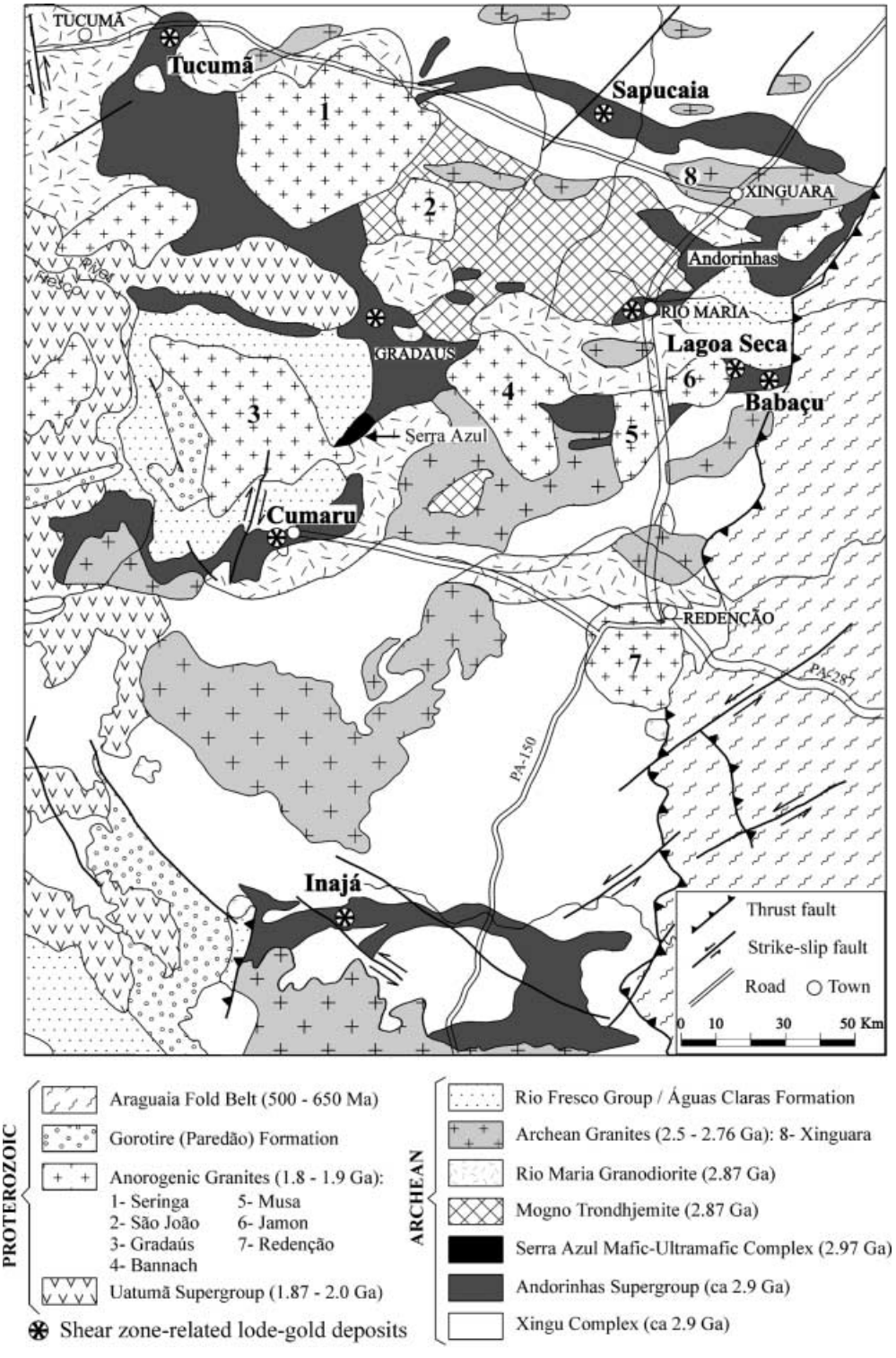

Fig. 8 Gold deposits of the Rio Maria Granitoid–Greenstone Terrane (adapted from Schobbenhaus et al. 1981; Docegeo 1988; Faraco et al. 1996)

the Lagoa Seca Group (Souza 1999). Cumaru is a somewhat distinct deposit because it also exhibits a strong influence of a granodiorite intrusion. The copper–gold ± tungsten subtype is represented by the Águas Claras deposit (Fig. 4), which, contrary to the orogenic gold deposits, has been formed in an extensional tectonic environment.

Sapucaia deposit

The Sapucaia greenstone belt (Fig. 9) forms a WNW-trending ridge underlain by supercrustal rocks and controlled by a major dextral shear zone (Oliveira and Leonardos 1990). According to these authors, the Sapucaia shear zone is made up of a complex array of

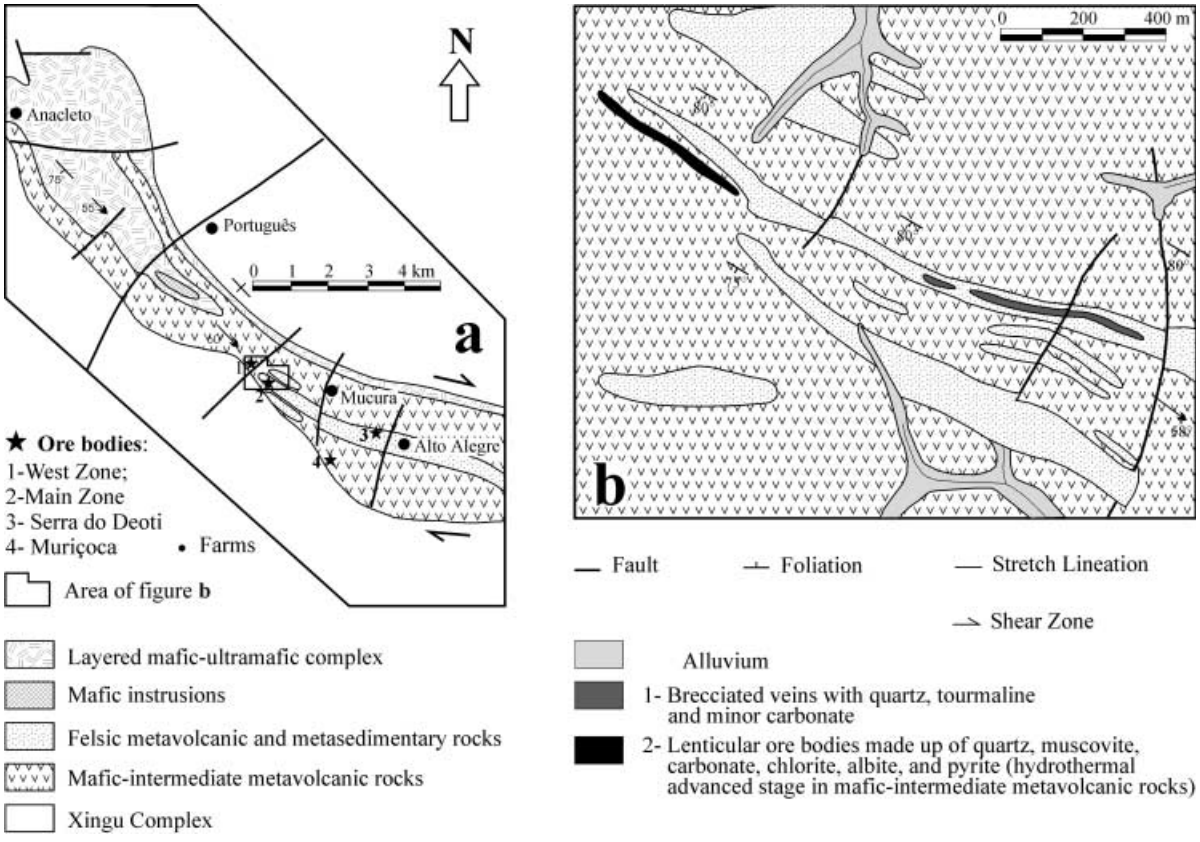

Fig. 9 The Sapucaia deposit. **a** Geological outline of the central part of the Sapucaia greenstone belt. **b** Geological map of the Main zone and West zone orebodies (adapted from Oliveira et al. 1995)

conjugate shears that cut both the greenstone sequence and the surrounding granitic terranes, and where intense brittle–ductile shearing has taken place. The shear zone has an anastomosing pattern, both on regional and smaller scales, and regionally is characterized by low-strain pods within a broader area of intensely deformed rocks. In addition to the mylonitic to ultramylonic foliation, S–C surfaces are marked by a succession of cataclastic and mylonitic bands.

The main orebodies are quartz veins, which are as wide as a few metres and as long as 400 m. These veins are parallel to the trace of the shear zone and are controlled by D-Riedel faults. Extension (gash) veins also occur, but are barren or only weakly mineralized. The characteristic early alteration assemblage consists of clinochlore, carbonate minerals, albite and muscovite. Subsequent alteration included additional carbonatization, partial disappearance of clinochlore and epidote, formation of albite–carbonate and chamosite–sericite assemblages in the mafic and intermediate volcanic rocks, and growth of tourmaline in the felsic and intermediate rocks. Late-stage alteration is marked by a quartz–pyrite assemblage in the mafic and intermediate rocks and by muscovite–carbonate and quartz–tourmaline assemblages in the felsic rocks. Gold is very fine-grained and occurs as free particles, occluded within euhedral pyrite grains or as coatings on the surface of tourmaline crystals (Oliveira and Leonardos 1990). Magnetite and ilmenite are more abundant than sulfide minerals which are mainly pyrite with minor chalcopyrite, pyrrhotite, mackinawite and millerite. There are no data on gold resources.

Coexisting oxygen isotope pairs for quartz ($\delta^{18}O_{SMOW} = 10.3–11.5‰$) and calcite ($\delta^{18}O_{SMOW} = 8.3–10.1‰$) allow calculated temperatures ranging from 350 to 170°C for the hydrothermal fluid (Oliveira et al. 1995). Because ore fluids are assumed to be at least partly of metamorphic origin, and a metamorphic temperature of 470–480°C was obtained from a quartz–magnetite pair from banded-iron formation, it is likely that the ore formation may have occurred at temperatures higher than 170–350°C range and this range might only reflect isotopic re-equilibration. The source of the ore fluids has been constrained by stable isotope compositions of carbon, oxygen and hydrogen in hydrothermal minerals. Based on the mean isotopic composition of hydrogen in chlorite ($\delta D_{SMOW} = -58‰$) and of carbon ($\delta^{13}C_{PDB} = -3‰$) and oxygen in the late stage calcite ($\delta^{18}O_{SMOW} = +9‰$), as well as on the initial strontium ratio ($^{87}Sr/^{86}Sr = 0.7155$) of this carbonate, the ore fluids suggested to be metamorphic or magmatic fluids or even a mixture of these fluids (Oliveira et al. 1995).

Cumaru deposit

The Cumaru gold deposit is hosted by a I-type, calc-alkaline 2.8 Ga granodiorite stock of volcanic arc affiliation

(Santos et al. 1998). This igneous body is a late tectonic pluton intruded into horse-tail dilation sites of the Serra Ruim shear zone, which transects the volcano-sedimentary rocks of the Archean Gradaús greenstone belt (Fig. 10). These rocks include flows, tuffs, and ignimbrites of felsic, intermediate and mafic composition, as well as banded iron-formations, clastic-chemical sedimentary units and minor ultramafic rocks, regionally metamorphosed mainly under greenschist facies conditions.

The Cumaru deposit is an auriferous quartz-vein swarm, chiefly within the north-western margin of the Cumaru stock, but also hosted by the felsic to intermediate volcanic rocks. The main lodes are 10-cm- to 1-m-wide quartz veins enclosed in extensional fractures and faults related to the Serra Ruim shear zone. Although the high-grade ore shoots (~10 g/t Au) are normally restricted to the thicker veins, stockwork arrays of veinlets also envelope the veins within a

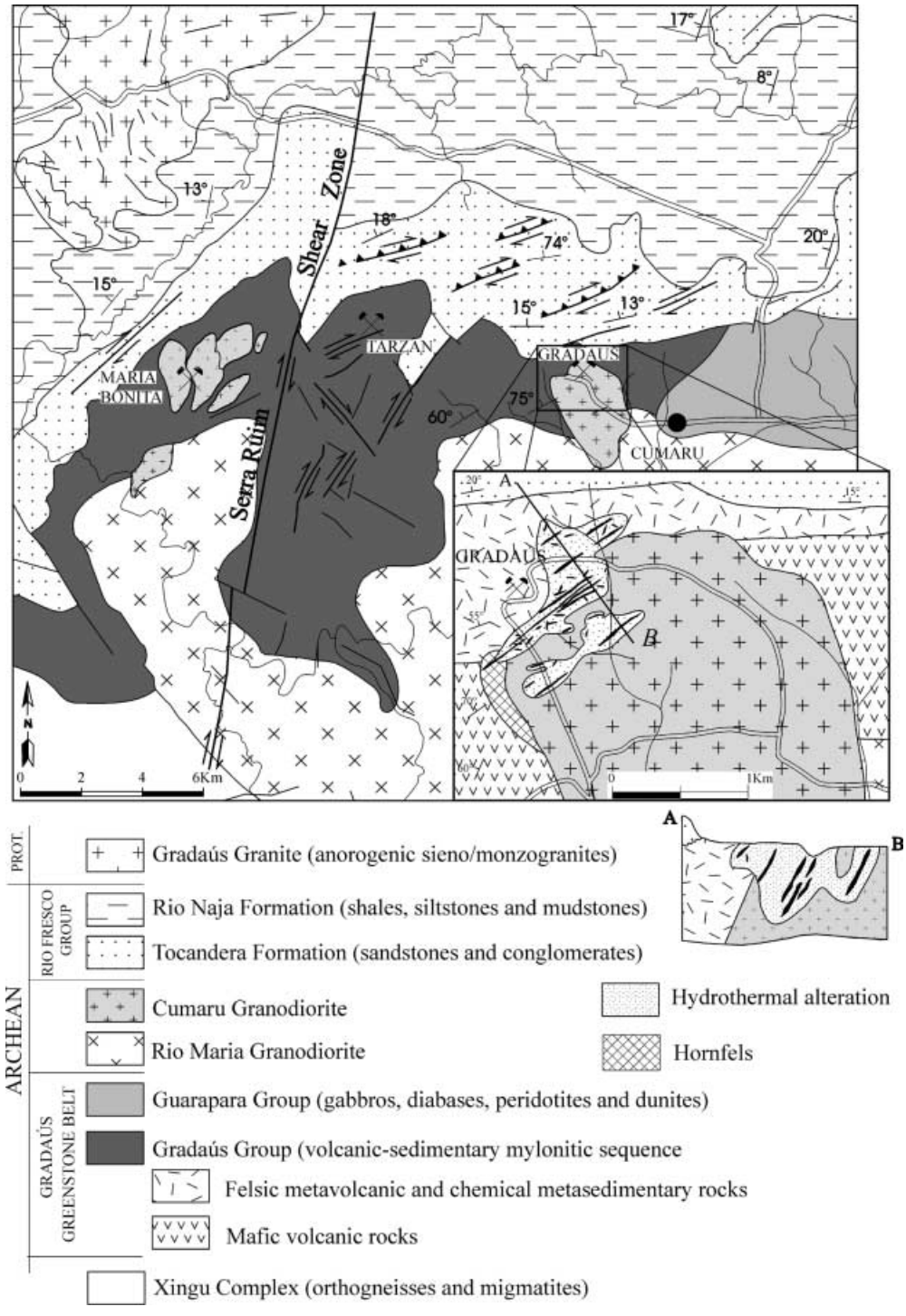

Fig. 10 Geological map of the southern flank of the Gradaús greenstone belt, showing the Cumaru gold deposit in detail (according to Santos 1995)

pervasively altered, brecciated quartz–sericite-rich rock with minor chlorite, epidote, pyrite, albite and calcite. Gold accompanies a sulfide assemblage, which is dominated by early pyrite, with minor chalcopyrite, bismuthinite and rare molybdenite. Within veins and altered wallrock, an interstitial oxidized assemblage (magnetite + hematite + later pyrite) fills the voids between early larger pyrite clasts (Santos, 1995; Santos et al. 1998). The Cumaru resource is about 17 t Au, with a mean grade of 10 g/t (Faraco et al. 1996).

Three kinds of fluids are identified in the Cumaru quartz veins (Santos and Leonardos 1995). An aqueous-carbonic fluid, which unmixed at the time of ore formation, is interpreted by these workers to be of metamorphic derivation and related to the development of the shear zone. Homogenization temperatures for these inclusions fall in the 210–280°C range, but some fluid inclusions decrepitated between 250 and 300°C before total homogenization was completed. Measurements of clathrate melting temperatures provide estimates of salinities of 19–20.5 wt% equiv. NaCl for the unmixed aqueous inclusions. Gold likely precipitated from this early aqueous-carbonic fluid, as evidenced by the very common occurrence of tiny gold-related sulfide minerals in the fluid inclusions. The second type of fluid comprises NaCl–KCl–$CaCl_2$ brines, which are considered to have evolved via magmatic exsolution. Dissolution temperatures of daughter minerals vary from 230 to 270°C, corresponding to salinities of between 34 and 36 wt% equiv. NaCl. The youngest fluids are low-salinity aqueous solutions ($Tm_{ice} = 0$ to –6°C) that are probably meteoric water. The T–P conditions of the gold deposition, constrained by chlorite geothermometry and isochoric calculations from fluid inclusion microthermometric data range from 300–350°C and 1.3–3.8 kbar (Santos et al. 1998). Fluid immiscibility and wallrock sulfidation may both have been important for ore deposition.

Stable isotope data are interpreted by Santos et al. (1988) to suggest that the aqueous-carbonic fluid mixed with an evolving magmatic brine during gold deposition. Santos et al. (1988) note that the features of the Cumaru gold deposit are similar to both Archean greenstone-hosted shear zone-related lode-gold deposits and to porphyry-style mineralization typical of Phanerozoic magmatic arcs. Such characteristics led them to suggest a hybrid genetic model in which both fluid flow along the shear zone and from the granodiorite intrusion were involved in the genesis of the Cumaru gold deposit, which was then termed a 'lode-porphyry' gold deposit. However, the lack of a porphyritic igneous phase suggests this not to be the best possible terminology.

Águas Claras deposit

The Águas Claras deposit differs from the above orogenic gold deposits hosted in shear zones by (1) its formation in an extensional tectonic setting, (2) the abundance of chalcopyrite in the ore zones and (3) the apparent absence of carbonic fluids in the ore-forming hydrothermal system.

The Águas Claras copper–gold ± tungsten deposit is located approximately 5 km west of the 1.88-Ga Serra dos Carajás granite (Fig. 4). A steeply-dipping, NE-trending, brittle to brittle–ductile, dextral shear zone is the main structural feature in the deposit area. This zone can be traced for 3–4 km and is terminated to the north by the regional Carajás fault (Fig. 4). It cuts both rocks of the Águas Claras Formation and 2,645 ± 12 Ma gabbroic sills and dikes (Table 2), with offsets of more than 100 m in ore zones (Fig. 11).

The gold-bearing vein network, which lies within the shear zone, is about 20-m-wide at surface but narrows to 6 m at a depth of 250–300 m. Its minimum lateral extent is estimated at 400 m and individual veins have straight to irregular borders and are tens of millimetres to a few centimetres wide. Chloritization and sericitization are the most characteristic alteration types adjacent to the veins, with less pervasive tourmalinization, silicification, carbonatization and kaolinization (Silva and Villas 1998). Epidote and albite are also present, but are probably pre-ore secondary phases related to the gabbroic intrusions (Barros et al. 1994a).

The veins show a variety of geometries and filling textures (Silva and Villas 1998). They are mainly composed of quartz, but chlorite, tourmaline, white mica, kaolinite, carbonate and sulfide minerals, fluorite, epidote and albite may be present in various combinations, the last two, however, being confined to the veins/veinlets that cut the mafic rocks. Monomineralic veinlets of siderite cut older structures and probably represent the final stage of the Águas Claras hydrothermal system. The sulfide minerals, which tend to occupy the central parts of the veins, generally amount to 5–10% of the vein material, but locally may reach 80%. Chalcopyrite, pyrite, sphalerite and arsenopyrite, in order of abundance, are the main sulfide minerals. Galena, pyrrhotite, cobaltite, bismuthinite, stannite and tennantite are present as subordinate phases (Soares et al. 1994). Magnetite and hematite occur in similar amounts (6–7%), whereas ferberite is a minor constituent (< 2%). A general paragenetic sequence for the ore deposition is pyrite + arsenopyrite + cobaltite + magnetite + hematite → chalcopyrite → ferberite. Pyrite–ferberite-bearing veinlets, however, cut chalcopyrite grains reflecting subsequent fracturing of pre-existing ore.

Gold is fine grained and is electrum (75% Au and 25% Ag). It occurs as (1) inclusions in arsenopyrite grains, (2) at pyrite–chalcopyrite contacts and (3) as isolated particles in chalcopyrite aggregates (Soares et al. 1994). Ore resources are estimated at approximately 9,550,000 t with an average gold content of 2.43 g/t (C.A. Medeiros Filho, personal communication 1996). Higher gold values occur in the lateritic or gossan cover.

Fluid inclusion studies (Silva 1996a) reveal that the fluids associated with the Águas Claras hydrothermal

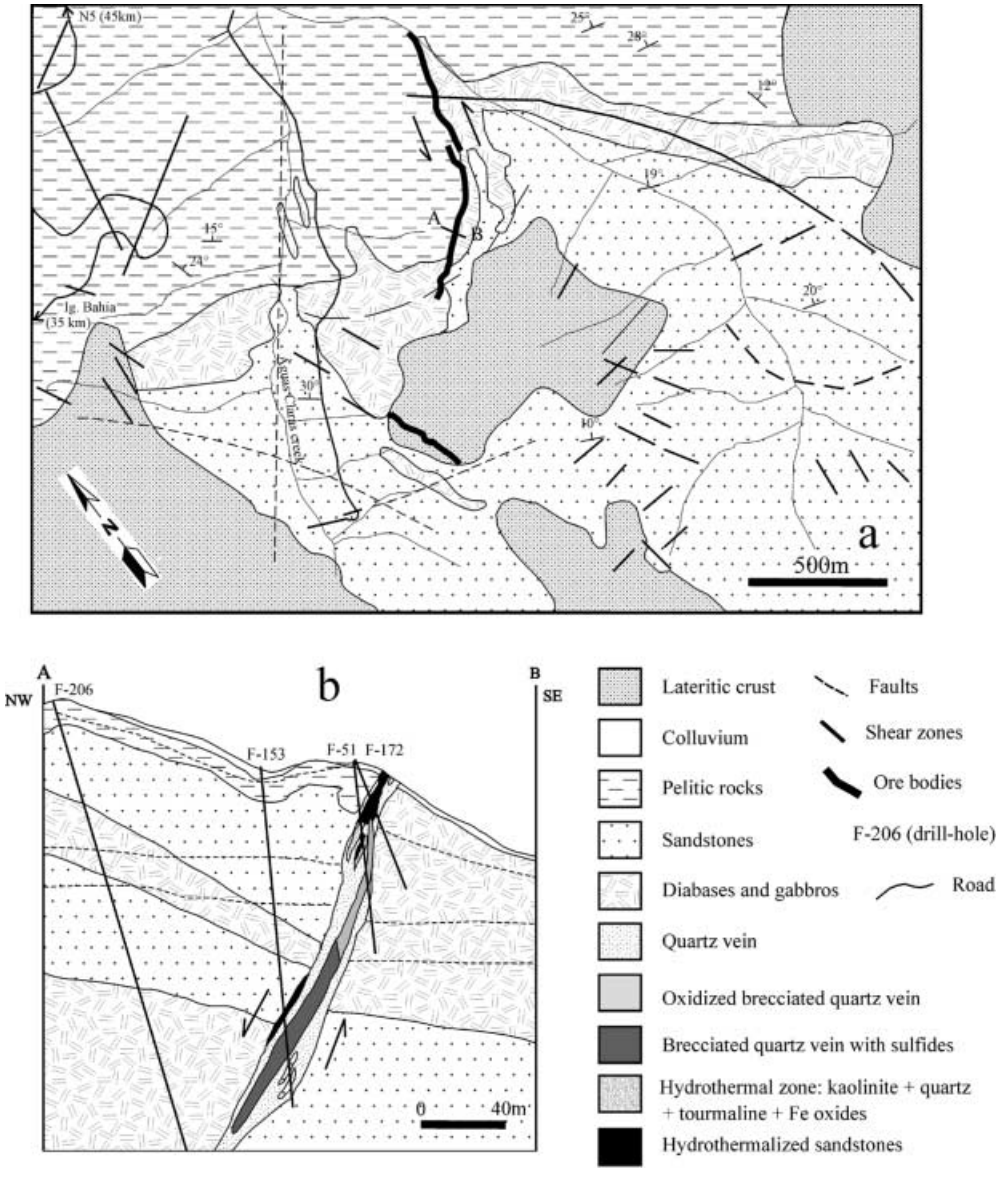

Fig. 11 **a** Geological map of the Águas Claras deposit and **b** cross section of one mineralized quartz lode (source: Docegeo, internal report)

system were aqueous solutions containing NaCl, $CaCl_2$ and $MgCl_2$ as major solutes. Homogenization temperature ranges of 160–360 and 100–360°C have been obtained, respectively, for highly saline (30–45 wt% NaCl equiv.) and dilute to moderately saline fluids (0.5–23.5 wt% NaCl equiv.).

Type IV (sedimentary rock-hosted gold–PGE deposits)

Serra Pelada deposit

The Serra Pelada or Serra Leste deposit (Fig. 4) is the only gold mineralization spatially associated with carbonate rocks in the CMP. It possesses some intrinsic characteristics that render it unique in the ISB (Meireles et al. 1982; Meireles and Silva 1988; Tallarico et al. 2000a). First, whereas the other deposits are Cu–Au-rich, the Serra Pelada deposit is apparently poor in ore-stage sulfide minerals. Second, folds are the most important structural controls of the mineralization, which is mainly concentrated in the hinge of an asymmetrical plunging syncline. Third, gold is palladium-rich (1–10%, locally as much as 50% Pd) and occurs as fine particles disseminated in pelitic rocks at sites of strong manganese metasomatism.

The Serra Pelada garimpo became famous worldwide because of the legion of approximately 40,000 gold diggers that moved into the area in the early 1980s, a migration that typifies the search for minerals in the Amazon region. From 1980 to 1984, 32.6 t of gold, including gold nuggets as large as 62 kg, were produced from alluvial deposits and from the supergene enriched mantle (Meireles and Silva 1988). Despite penetrating to depths of 300–350 m, exploration drill holes barely reached the base of the weathering profile, thus re-

stricting most geological investigation to the oxidized zone. A low-grade metamorphic, folded clastic-chemical sequence hosts the gold mineralization. It overlies rocks of the Rio Novo Group and is correlated with the Rio Fresco Group (Table 1). These two lithostratigraphic units have not been dated yet, but most geological evidence points to their formation in the Archean. The former is intruded by the 2,763 ± 7 Ma Estrela granitoid and the latter is interpreted to be correlated with the Águas Claras Formation, which is cut by 2,645 ± 12 Ma gabbroic sills and dikes (Table 2).

The folded sequence includes conglomeratic to psammitic rocks at the bottom, and carbonate and pelitic rocks towards the top. Some metasandstones are manganese-rich, but occur only locally. Grey to black metasiltstone layers, of variable thickness, are intercalated with metasandstones and red metasiltstones. These darker pelitic units owe their colour to amorphous carbon (Tallarico et al. 2000a) and they become progressively scarcer towards the top of the sequence where the red metasiltstones are dominant. Sericite is the only significant metamorphic mineral in these clastic rocks. The underlying carbonate rocks are represented by dolomitic marbles, which, according to those authors, are composed of quartz grains (1–30 wt%) and rare clasts of iron formation and quartzite in a granoblastic matrix made up, in a general decreasing order of abundance, of dolomite, actinolite, chlorite, biotite, calcite, talc and rare diopside. The dolomitic marble is intruded by dioritic rocks at depths of 300–350 m in the south-western corner of the deposit area. Details of these intrusions remain unknown (Tallarico et al. 2000a).

The hydrothermal assemblages are highly dependent on the nature of the host rock (Tallarico et al. 2000a). The quartz + chlorite ± calcite ± tourmaline ± pyrite ± chalcopyrite association occurs both in veins that transect the foliation of metasiltstones and as a matrix of breccias. Euhedral spessartite poikiloblasts disrupt foliation planes indicating post-tectonic growth related to a thermal event. In the dolomitic marble, widespread chlorite has replaced actinolite, talc and biotite. Pyrrhotite, pyrite and chalcopyrite coexist with chlorite. Magnetite and muscovite are present in amounts that vary greatly, but do not exceed 20–25 wt%. Tourmaline, titanite, allanite, epidote, monazite, apatite, molybdenite, galena and thorite occur as accessory phases. The dioritic rocks are altered to albite, sericite, quartz, chlorite, rutile and carbonate minerals, as well as cut by veins consisting of quartz, epidote, chlorite, sericite and sulfide minerals.

The Serra Pelada orebodies lie in the hinge of a recumbent syncline, appearing as an inverted saddle-reef, at the contact between the dolomitic marble and the carbonaceous metasiltstones and enclosed by a 5- to 50-m-thick jasperoid layer (Fig. 12). These carbonaceous metasiltstones are the main host rocks to the gold–(palladium–platinum) mineralization. Mineralogical studies of these rocks (Tallarico et al. 2000a) show that they consist of amorphous carbon (1–10 wt%), quartz (10–60 wt%), sericite (1–30 wt%), kaolinite (1–20 wt%), hematite (1–40 wt%), goethite (1–15wt%) and Mn-oxides (1–15 wt%), with traces of sulfide minerals (pyrite, chalcopyrite, arsenopyrite, covellite, bornite, galena, millerite, pentlandite, carrollite and siegenite), tourmaline, carbonate minerals, chlorite and magnetite. According to Tallarico et al (2000a), the present-day trace amounts of sulfide minerals may be the result of intense supergene oxidation. However, were these minerals more abundant, evidence of a gossan cover, until now unreported, would be expected at the surface. Palladium occurs both as natural alloys (average 94 wt% Au, 3 wt% Ag, 3 wt% Pd) and as atheneite and potarite. Isoferroplatinum is the only platinum mineral so far identified. Gold occurs either as alloys or as free particles with diameters in the range of 4–60 mm (Tallarico et al. 2000a).

The metasedimentary sequence has been disturbed by folding and faulting that generated channelways for mineralizing fluids. Highly permeable zones related to fold hinges, tectonic breccias and fault planes were important structural traps for gold deposition. Gold has been upgraded by supergene processes that were also responsible for the decalcification of the dolomitic marble and the consequent formation of collapse breccias (Tallarico et al. 2000a). Recent reserve calculations for primary ore yield a little more than 30 t of Au (Viveiros 1999). No data are available for the PGE resources.

Summary

The overprint of several geological events on most deposits and the scarcity of isotopic, geochemical and fluid data for most of the Carajás gold deposits make the classification presented here a preliminary and tentative one. However, despite these drawbacks, this taxonomic scheme is an attempt to systematize the gold deposits of the region in terms that will be of assistance to future exploration programmes. The Archean metavolcano-sedimentary rocks and the overlying sedimentary sequences are important targets, particularly where folded, cut by shear zones, and/or intruded by Archean granitoids. It is important to note that the Fe-oxide-poor Cu ± Au and Fe-oxide–Cu–Au–U–REE deposits have been formed within metavolcano-sedimentary sequences, regardless of the presence of the Palaeoproterozoic granitoids. At places where these granitoids occur, but intrude units other than metavolcano-sedimentary sequences, those types of deposits have not yet been identified in Carajás. This makes it unlikely that these granitoids were the source for copper and perhaps gold, although they certainly caused some redistribution of pre-existing ores. The orogenic gold deposits are characteristic of the RMGGT and have been not recognized to date in

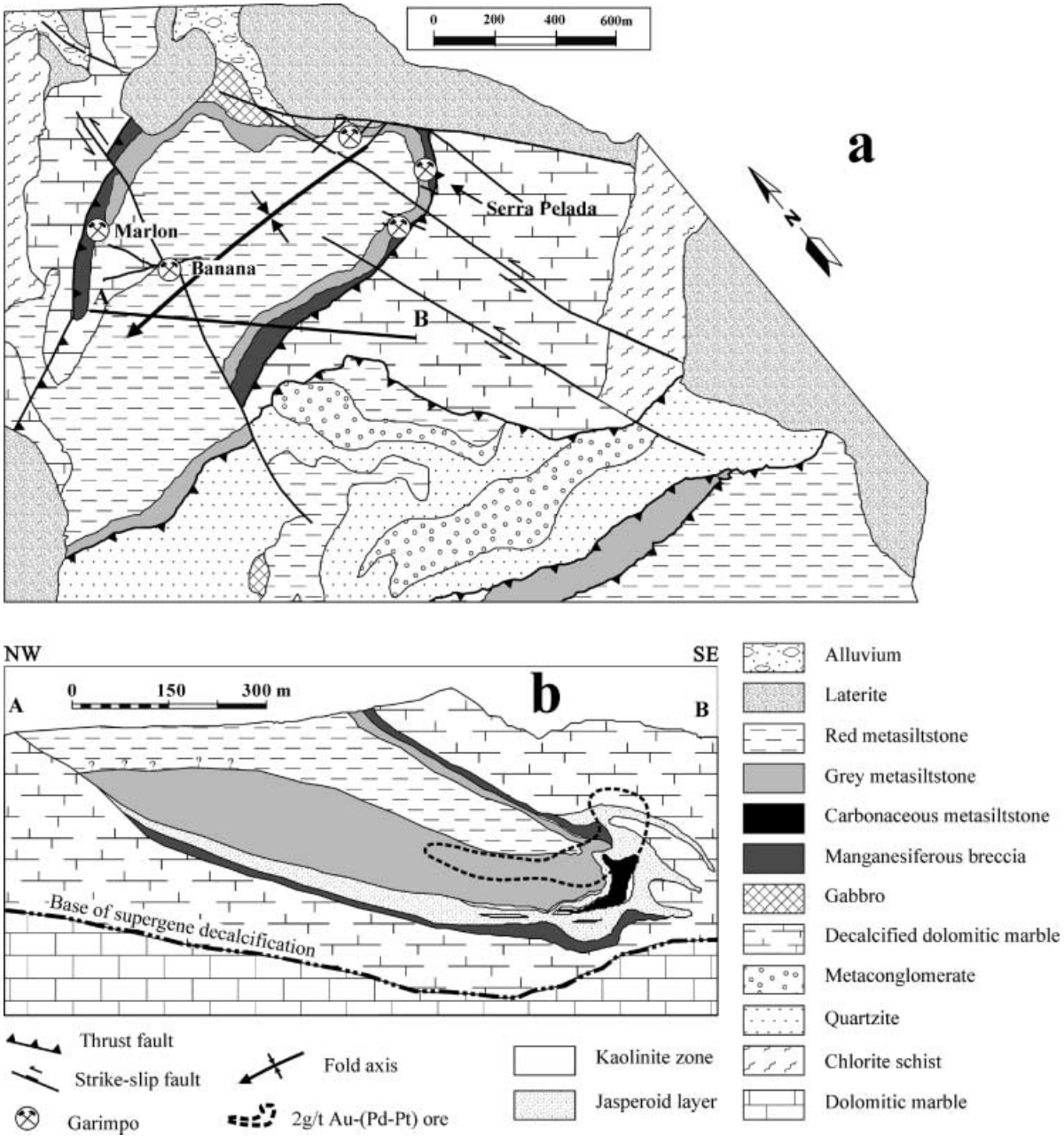

Fig. 12 **a** Geological map and **b** cross section *A–B* of the Serra Leste or Serra Pelada Au–(Pd–Pt) mineralization (modified from Talarico et al. 2000a)

the ISB. They are related to shear zones that cut and alter Archean greenstone belts, granitoids and metasedimentary rocks. The Cu–Au ± W vein deposits are also related to shear zones, but have formed in a tectonically distinct setting that is more typical of the Carajás basin evolution. A sedimentary rock-hosted gold- and PGE-rich deposit has been recognized only in the ISB. Its identification in rocks of the extensive Rio Fresco Group makes this unit an important target, especially where carbon-bearing pelitic and carbonate rocks have been folded and sheared.

Constraints on ages of gold deposits

Indirect constraints

The host rocks for all Carajás hypogene gold deposits are Archean in age (Table 2). As discussed above, the Palaeoproterozoic granitoids are unlikely sources for copper and gold mineralization in the CMP. In the RMGGT, undeformed dikes that intrude both the mineralized rocks and the Rio Maria granodiorite are thought to have resulted from the same thermo-tectonic event responsible for the regional anorogenic magmatism. One of these dikes, of diabase composition, yields a K–Ar age of 1,802 ± 22 Ma, which is interpreted to be close to its true crystallization age (Silva et al. 1996).

Consequently, the mineralizing events can be broadly bracketed within the interval from 2.9–1.9 Ga. A more precise age estimate for the orogenic gold deposits is available from the Cumaru deposit. Rubidium–Sr dates on hydrothermal white mica yield ages ranging from 2,551 to 2,450 Ma (Pereira 1992), which can be taken as the minimum age of both the shearing and associated gold mineralization, with an upper age limit being the 2.82 Ga Cumaru granodiorite host rocks.

In the ISB, the relationships between the main structures, granitic magmatism, and gold deposits still need to be better defined. For example, if the shear zones are secondary features of the regional WNW-trending Carajás fault, which is cut by the Serra dos Carajás granite, then the Águas Claras Cu–Au mineralization must be older than 1.88 Ga. On the other hand, if they are a product of the extensional tectonic event that triggered anorogenic magmatism, this mineralization could be contemporaneous with, or slightly younger, than it. Another possibility is the occurrence of a shearing event anytime between 2.8 and 1.9 Ga. In this regard, the 2,581–2,479 Ma interval has been interpreted as the latest reactivation of a WNW-trending dextral shear system, which might have given rise to the Carajás transtensional basin (Machado et al. 1991). In the ISB, this interval could be even greater, as indicated by a recent U–Pb date of 2,362 ± 19 Ma on apatite porphyroblasts from the Serra Verde deposit (Table 4), which has been interpreted to be the age of the associated shearing event (Felipe Reis, personal communication 2000).

The spatially-related dioritic rocks are inferred to have a genetic link with the Cristalino copper–gold mineralization (Huhn et al. 1999b). Thus, the Pb–Pb crystallization age of 2,738 ± 6 Ma (Table 1) may approximate this mineralization. Available geological data from the Serra Pelada deposit indicate that the gold mineralization post-dates 2,645 Ma, the minimum age of the Águas Claras Formation /Rio Fresco Group (Table 1).

Direct constraints

Attempts to date the Carajás deposits are relatively recent (Pereira 1992; Mougeot et al. 1996; Mellito and Tassinari 1998) with U–Pb, Pb–Pb and Rb–Sr analyses being undertaken on samples from the Igarapé Bahia, Igarapé Pojuca, Águas Claras, Formiga (near Serra Pelada), Serra Verde, Igarapé Salobo and Cumaru deposits. The resulting data are shown in Table 4.

Based on U–Pb and Pb–Pb isotope studies, Mougeot et al. (1996) determined an age of 2,850 ± 65 Ma for the Igarapé Bahia deposit using the Stacey–Kramers model in a uranium-enriched domain. They also proposed a stage of lead evolution between 3,700 and 2,800 Ma by analysing sulfide minerals from both the Águas Claras Formation and gabbroic sills and dikes. They recorded evidence of lead remobilization at 2,060 and 1,880 Ma in many gold occurrences in the ISB. The 1,880 Ma value was considered to be related to the anorogenic granite magmatism.

At the Igarapé Bahia deposit, isotopic data for chalcopyrite from the breccias (Pb–Pb isochron) and for zircons from pyroclastic rocks (Pb–Pb evaporation technique) show comparable ages (Table 4) within the range of analytical error. As the metapyroclastic rocks overlie the mineralized breccias, the age difference could be, in part, explained in terms of their stratigraphic position. The 2,768 ± 29 Ma value (chalcopyrite) is also equivalent to the ages of other metavolcano-sedimentary sequences of the ISB, namely the Igarapé Salobo (2,761 ± 3 Ma) and Grão Pará (2,759 ± 2 Ma) groups

Table 4 Available ages for some Carajás gold deposits and their corresponding host rocks. *ZR* Zircon

Deposit	Host rocks				Mineralization			
	Rock type	Age (Ma)	Method	Source[a]	Mineral	Age (Ma)	Method	Source[a]
Aguas Claras	Intrusive gabbroic sills	2,645 ± 12	Pb–Pb (ZR)	1	Chalcopyrite	1,880	U–Pb	2
						2,358 ± 42	Pb–Pb	3
Cumaru	Granodiorite	2,817 ± 4	Pb–Pb (ZR)	4	White mica	2,551–2,450	Rb–Sr	5
Serra Verde	Mafic metavolcanics	2,747 ± 120	Pb–Pb	6	Apatite	2,362 ± 19	U–Pb	6
					Chalcopyrite/ molybdenite	2,760 ± 77	Pb–Pb	6
Igarapé Salobo	Amphibolite	2,761 ± 3	U–Pb (ZR)	7	Sulfides/magnetite	2,200–2,000	Pb–Pb	8
						2,850–2,750	Pb–Pb	8
Igarapé Bahia	Metapyroclastic rocks[b]	2,747 ± 2	Pb–Pb (ZR)	9	Chalcopyrite	1,880	U–Pb	2
						2,768 ± 29	Pb–Pb	9
						2,850 ± 65	U–Pb	2

[a] *1* Dias et al. (1996); *2* Mougeot et al. (1996); *3* Cintia G. da Silva (personal communication 2000); *4* Lafon and Scheller (1994); *5* Pereira (1992); *6* Felipe N. Reis (personal communication 2000); *7* Machado et al. (1991); *8* Mellito and Tassinari (1998); *9* Moacir B. Macambira (personal communication 2000)

[b] Overlying the mineralized breccias

with which the Igarapé Bahia Group has been correlated. The available data suggest that both host rocks and mineralization at the Igarapé Bahia deposit are coeval. In this context, the age of 2,850 ± 65 Ma obtained by Mougeot et al. (1996) for the primary sulfide mineralization is quite discrepant to warrant any geological significance.

Lead isotope studies on chalcopyrite from the main ore zone of the Aguas Claras deposit yielded an age of 2,358 ± 42 Ma (Table 4), which can be interpreted in three different ways. It could represent the true age of the copper–gold mineralization. Alternatively, because of the proximity of the 1.88-Ga Serra dos Carajás granite, it could represent Archean ore sulfide that was isotopically reset, in agreement with the age of 1,880 Ma obtained by Mougeot et al. (1996). The third possibility implies mixing of lead inherited from the host rocks. However, inclusions of uraninite in sulfide minerals and the high values of radiogenic lead in the sulfides favour this lead to be a product of the uranium decay, rather than inheritance.

The Pb–Pb analyses for sulfide minerals and magnetite (Mellito and Tassinari 1998) from the Igarapé Salobo deposit distinguish two mineralization periods: (1) 2.85–2.75 Ga for the main copper–gold mineralization; and (2) 2.2–2.1 Ga for gold remobilization by fluids related to Proterozoic metamorphism and/or magmatism. The lower limit of the first period is consistent with the age of the host rocks (Igarapé Salobo Group) and strongly suggests contemporaneity between sedimentation and ore formation. The younger ages (2.2–2.1 Ga) may be related to isotopic re-equilibration caused by intrusions of the Young Salobo granite.

Isotopic studies on the Serra Verde rocks and ores (Felipe Reis, personal communication 2000) allow a preliminary assessment of the temporal evolution of the deposit. As the 2,763 ± 7 Ma Estrela granite (Table 2) is intrusive into the rocks of the Rio Novo Group and the sulfide lenses are thermally metamorphosed, the copper–gold mineralization must be older than the magmatism. In addition, the ages of the host volcanic rocks and sulfide minerals (2,747 ± 120 and 2,760 ± 77 Ma, respectively, Table 4) are, despite the large analytical error, fairly coincident, indicating contemporaneity between the host rock formation and mineralizing events. In fact, the deposition of the host rocks, the precipitation of the sulfide minerals and gold, and the granitic intrusion appear to have occurred in the same short period of time. Unfortunately, the precision of some of the isotopic methods used is still inadequate to place better age constraints on these different events. In fact, these isotope studies also indicate an age of 2,509 ± 85 Ma defined on a $^{207}Pb/^{204}Pb$ versus $^{206}Pb/^{204}Pb$ plot, by the alignment of points derived from analyses of molybdenite and chalcopyrite. A 2,362 ± 19 Ma U–Pb age on apatite porphyroblasts (Table 4) is interpreted to reflect isotopic resetting during a late shearing event.

Genetic models

Fe-oxide-poor Cu ± Au deposits

Several lines of evidence support formation of the Serra Verde deposit prior to the emplacement of the syntectonic Estrela granitoid. Diagnostic metamorphic textures have overprinted the ores, which are also cut by 1- to 2-cm-thick veins composed of hexagonal pyrrhotite that resulted from thermal overprinting of pre-existing iron-rich sulfide minerals. Magnesium–hornblende porphyroblasts in the chalcopyritic matrix are compositionally different from amphibole in the Estrela granitoid (Barros 1997) and they may represent thermally transformed seafloor hydrothermal mafic minerals. Tourmaline in the metasedimentary host rocks and granitoid are also chemically distinct, the latter being much richer in iron. The Estrela body is relatively unmineralized and unaltered, showing only some local chalcopyrite disseminations and erratically distributed epidote-rich assemblages. All these observations tend to rule out the Estrela granite as a potential metal source for the Serra Verde mineralization.

Unfortunately, the available geochronological data show large errors and the temporal relationships between the host rocks and mineralization are still poorly constrained. Accepting, however, that the sulfide and gold mineralization is syngenetic, the following arguments favour a volcanogenic origin: (1) the volcanosedimentary nature of the host sequence, consisting of clastic (arkoses and greywackes) and chemical (cherts and iron-formations) units intercalated with basaltic rocks; (2) the general mode of occurrence of the sulfide minerals as massive lenses conformable to the stratification of the host rocks; and (3) the presence of quartz- and chlorite-rich rocks and dravitic tourmalinites associated with the sulfide lenses.

Accordingly, the Serra Verde deposit could fit the volcanogenic massive sulfide (VMS) category, although the paucity of iron–sulfide minerals is unusual. It is possible to envisage a system extremely rich in copper, such that chalcopyrite predominates, if a magmatic fluid source at depth was exceptionally copper-rich (Fig. 13). It is possible that both phosphorus and titanium were similarly derived and led to precipitation of apatite and ilmenite, respectively, on the seafloor. Links to specific magmatic bodies remain to be demonstrated, although subvolcanic intrusions similar to the sulfide-, apatite- and titanite-bearing Borrachudo body in the vicinity of the Cristalino deposit (Farias and Villas 1996) could be present.

Fe-Oxide–Cu–Au–U–REE deposits

This type of deposit is still poorly understood in the Carajás region. At the Cristalino deposit, geological data are limited and at the Igarapé Salobo and Igarapé

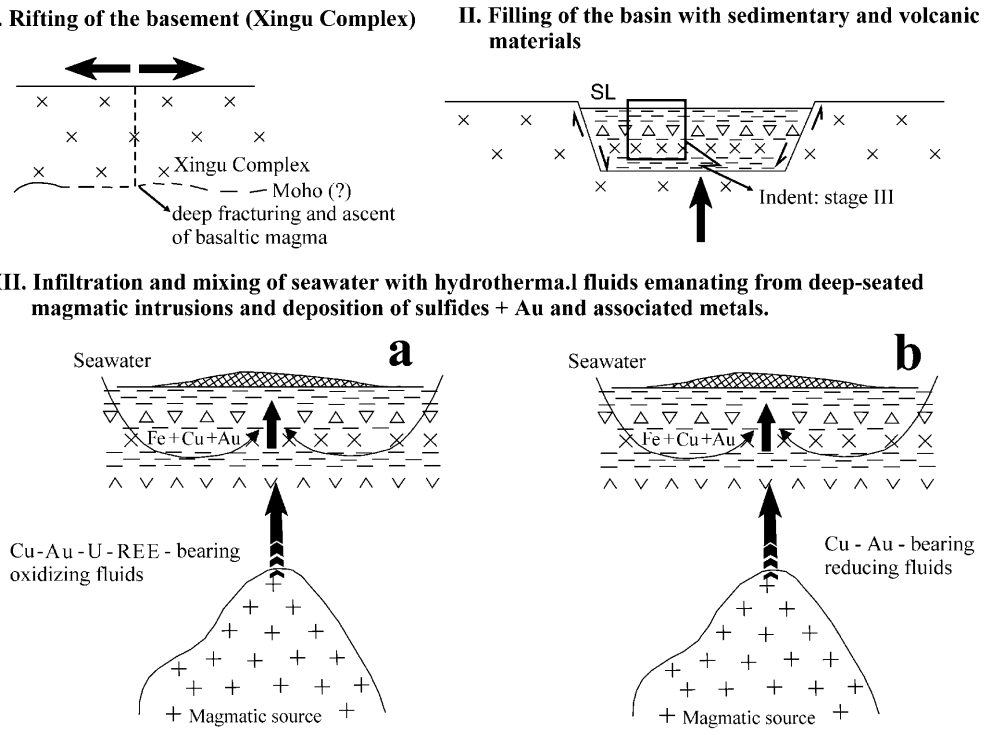

Fig. 13 Idealized model for the formation of the Carajás syngenetic Cu–Au ± U–REE deposits. **a** Igarapé Salobo and Igarapé Bahia deposits. **b** Serra Verde deposit

Bahia deposits, interpretations of data are contradictory. Different views argue either for an epigenetic Fe-oxide–Cu–Au–U–REE Olympic Dam-type model or a volcanogenic model, the latter accepting that a later magmatic hydrothermal event may have accounted for the anomalous concentrations of uranium, REE, and even some of the gold. Critical data, such as stable isotopic compositions, are still lacking and mineralization ages are insufficient to put firm constraints on either genetic model.

Similarities of the Igarapé Salobo and Igarapé Bahia deposits with the Australian Olympic Dam deposit include, in addition to the metal suite, the alteration styles, fluid compositions and tectonic environment (Huhn and Nascimento 1997; Oliveira et al. 1998; Tallarico et al. 1998; Lindenmayer and Teixeira 1999; Soares et al. 1999; Tazava 1999; Tallarico et al. 2000b).

Those who favour a volcanogenic-exhalative origin (Ferreira Filho 1985; Althoff et al. 1994; Almada 1998; Almada and Villas 1999) note that the magmatic systems associated with the Igarapé Bahia and Igarapé Salobo deposits are dominated by volcanic, rather than plutonic, rocks. They also argue that the orebodies are generally conformable with host rocks and that all copper–gold mineralization in Carajás is confined to the supracrustal metavolcano-sedimentary sequences of the ISB. The Archean mafic volcanic rocks of the Igarapé Salobo and Igarapé Bahia groups are basaltic in composition and were formed during rifting in the Carajás basement. Globally, such an environment was very propitious for the accumulation of banded iron formations as well as auriferous exhalative massive sulfide deposits (Poulsen et al. 1992; Herzig et al. 1993; Kerswill 1993; Hannington et al. 1999; Roth et al. 1999).

A third group of workers defend a multi-stage evolution for both deposits in which a magnetite-rich syngenetic copper deposit was overprinted by an assemblage rich in gold, uranium, molybdenum, fluorine and REE during a later epigenetic magmatic hydrothermal event (Lindenmayer and Fyfe 1994; Réquia et al. 1995; Tallarico et al. 2000b).

Some diagnostic features of the Proterozoic iron oxide (Cu–Au–U–REE) deposit types (Hitzman et al. 1992; Oreskes and Hitzman 1993) have not yet been described for the Archean Igarapé Salobo and Igarapé Bahia deposits. These include (1) the common presence of felsic to intermediate volcanic to plutonic host rocks, although the mineralization itself may be related to deep-seated magmatism; (2) the mineral zoning defined, from deeper to shallower levels, by magnetite → hematite and pyrite → chalcopyrite → bornite; (3) distinct sodic and potassic alteration zones; (4) the general dominance of pyrite over other sulfide minerals in magnetite-rich deposits; and (5) the common paragenetic sequence from an earlier magnetite + pyrite assemblage to a later hematite or hematite + Cu–Fe–sulfide assemblage. Notwithstanding, at the Igarapé Salobo deposit, features such as the high REE concentrations in the mineralized iron-formations, the lack of sedimentary banding, and the gradational contacts between the aluminium-rich metasedimentary rocks and the iron formations have been considered as indicative of metasomatic replacement of the host rocks (Lindenmayer and Teixeira 1999). On the other hand, some of these iron formations could have been true banded iron

formations, with the silica-rich bands having been destroyed and mostly consumed in the formation of fayalite, grunerite and almandine during metamorphism.

Other features that favour a volcanogenic-exhalative origin are recognized mainly in the Igarapé Bahia deposit and include (1) widespread chloritization, (2) thin stratiform massive sulfide beds interlayered with metasedimentary units and (3) thick massive Cu–Fe–sulfide lenses in the breccias (Alemão orebody). Furthermore, the stratigraphic position of the mineralized breccias, as a persistent contact marker between the mafic metavolcanic rocks and the metasedimentary–metapyroclastic rocks, constitutes strong evidence that these breccias are part of, rather than intrusive bodies into, the Igarapé Bahia Group. Also, the absence of unambiguous lithoclasts derived from the overlying rock pile and the presence of massive sulfide clasts in a conglomerate in the overlying metasedimentary rocks are suggestive of an earlier formation of both the phreatic breccias and sulfide mineral masses. Also the mineralization in the overlying Archean Águas Claras Formation, in addition to being weak and local, is characterized by magnetite-free and sulfide-rich veinlets and, therefore, is mineralogically distinct from that of the underlying breccias.

Table 5 compares some characteristics of the Igarapé Salobo and Igarapé Bahia deposits with the epigenetic Olympic Dam and Starra deposits of South Australia. It is obvious that, despite the many similarities, they differ in several important aspects, especially the age and mode of occurrence of the mineralization and zoning.

Considering that (1) mineralization occurs at a given stratigraphic position or within a restricted range, (2) ore units are both stratiform and stratabound, (3) ore units are laterally generally uniform in thickness and grade, (4) the boundaries of high grade ore against barren rock are commonly sharp, (5) there is no upward or downward extension of the orebodies; (6) the mineralization in tectonic, post-depositional structures is different, particularly in terms of contrasting very low magnetite contents and (7) the sulfide mineral ages are more consistent with those of the host rocks than of any other rock occurring in the Carajás basin, a syngenetic mode of deposition is favoured in this paper for both the Igarapé Salobo and Igarapé Bahia deposits. Local perturbations in the lead isotopic system may account for

Table 5 Comparison of the Igarapé Salobo and Igarapé Bahia deposits with two Australian Cu–Au deposits. *Act* Actinolite; *All* allanite; *Anh* anhydrite; *Calc* calcite; *Ep* epidote; *Hast* hastingsite; *Moly* molybdenite; *Safl* saflorite; *Uran* uraninite. For other mineral abbreviations, see legend for Table 2

	Igarapé Salobo deposit[a]	Igarapé Bahia deposit[b]	Olympic Dam deposit[c]	Starra deposit[d]
Tectonic setting	Rift or island arcs	Rift-like extensional basin	Extensional grabens	Intracratonic rift
Host rocks/associated igneous rocks	Iron-formations/Old Salobo granite (2,573 Ma); Young Salobo granite (1,880 Ma)	Breccias of the Igarapé Bahia Gr/post-mineralization dioritic dikes	Heterolithic breccias/ granitic and felsic volcanic rocks	Ironstones; breccias/Gin Creek granite (1,740 Ma)
Age/structures	2,761 Ma/shear zones	> 2,747 Ma/fractures	1.85–1.60 Ga/stockworks	1,790–1,670 Ma /shear zone, Isoclinal folds
Mode of occurrence of ore	Discontinuous massive to foliated, concordant to subconcordant lenses	Disseminated to massive; veinlets	Interstitial grains in breccia matrix; microveinlets; replacement	Disseminations in discontinuous, mostly discordant bodies
Ore mineralogy/ associated metals	Bn, Cc, Cpy, Py, Au/ Ag, Mo, U, REE	Cpy, Py, ± Bn, Au, Uran, REE-minerals/ Co, Mo, P, Ba	Bn, Cc, Cpy, Py, Au, U- and REE-minerals/ Ag, Co, Ni, Te, As	Au, Py, Cpy, ± Bn, ± Cc
Alteration types	K-metasomatism, silicification, propylitization	Chloritization, carbonatization, ± biotitization, silicification, tourmalinization	Sericitization, haematitization, silicification	Na–Ca–metasomatism, K–Fe-(low S)-metaso matism, sulfidation, carbonatization
Parageneses	(Mag–Fa–Alm–Hast–Cpy) – (Bt–Qz–Ab–Mag–Bn–Tour–Grun)–(Chl –Ep–All–Cc–Fl–Uran–Calc –Moly–Au–Cpy–Safl)	(Chl–Qz–Mag–Py–Cpy–Au) – (Sid–Tour–Bn) – Cpy–Cv	(Mag–Py–Sid–Chl) – (Hem–Ser–Qz–Uran–Fl–REE–minerals–Cu–minerals)	(Ab–Scap–Act) – (Bt–Mag–Qz) – (Hem–Au–Anh–Calc–Py–Cpy–Chl–Ser)
Age of mineralization	> 2.75 Ga	2,768 ± 29 Ma	< 1.4 Ga	< 1,584 Ma
Zoning	Not observed	Not observed	Py → Cpy → Bn	Albite alteration over-printed by biotite
Hydrothermal fluids	Saline aqueous and carbonic	Saline aqueous and carbonic	Saline aqueous and carbon ic	Aqueous
Resources	1,100 Mt @ 0.86% Cu	Alemão body: 170 Mt @ 1.5% Cu, 0.8 g/t Au	2,000 Mt @ 0.6 g/t Au, 1.6% Cu[e], av. ΣREE = 5,000 ppm	7.4 Mt @ 3.8 g/t Au, 1.88% Cu

[a]Lindenmayer and Teixeira (1999)
[b]Almada and Villas (1999)
[c]Hitzman et al. (1992)
[d]Rotherham (1997)
[e]Oreskes and Einaudi (1990)

some Palaeoproterozoic ages obtained from these deposits (Mougeot et al. 1996; Mellito and Tassinari 1998).

The proposed genetic model (Fig. 13) is similar to that of the Serra Verde deposit. The major differences are in the redox conditions of the ore fluids and the nature of the magmatic sources. The nature of the hidden intrusions is highly speculative, although the anomalous contents of REE, uranium, fluorine, phosphorous and barium suggest an alkaline or even carbonatitic affinity. Archean carbonatites are not common, but they have been described in Canada, Finland and Greenland (Bell 1989; Villeneuve and Relf 1998). Copper could have come, at least in part, from a similar source. The negative $\delta^{13}C_{PDB}$ values of the breccia-hosted carbonates (Oliveira et al. 1998) support a mantle-derived carbon source. Given that the mineralization ages of the Igarapé Salobo ores are older than 2.75 Ga, the proximal 2,573 ± 2-Ma Old Salobo granite is unlikely to be the mineralizing intrusion.

The extreme dominance of copper-sulfides over iron-sulfides is a problem if the Igarapé Salobo and Igarapé Bahia deposits are to be placed in the volcanogenic category. It is conceivable to have a submarine environment where a hydrothermal system, rich in copper and iron, and with high Cu/Fe and f_{O2}/f_{S2} ratios, favoured the precipitation of copper sulfide minerals and magnetite instead of pyrite. Oxidized and H_2S-deficient fluids are assumed to have accounted for the formation of some volcanogenic copper-bearing oxide deposits (Davidson 1992), although more recent studies reinterpret these same deposits as epigenetic (Rotherham 1997; Adshead-Bell 1998). The high sulfidation assemblage of the Igarapé Salobo deposit (chalcocite + bornite ± chalcopyrite) contrasts with the low sulfidation assemblage of the Igarapé Bahia deposit (chalcopyrite ± bornite). This difference could be explained by their positions in the deposition basin, the Igarapé Salobo deposit being more distal and formed at shallower depths where magmatic intrusions would be emplaced closer to the seafloor in a VMS environment (Hannington et al. 1999).

Shear zone-related lode-gold deposits

In the Carajás region, brittle to brittle–ductile shear zones developed in metamorphic rocks and appear to have been sufficiently permeable to focus fluids from transpressive sites to transtensive sites. These fluids were capable of leaching metals from the metavolcano-sedimentary piles through which they passed. Carbon-bearing units appear to be more common in the greenstone belt sequences and may have been the main source for the CO_2 and/or CH_4 incorporated into gold-depositing fluids there. In fact, low-salinity aqueous-carbonic fluids were only identified in gold deposits in the RMGGT. These fluids are considered to be derived from the underlying crust, as postulated for the orogenic gold deposit model (Groves 1993; Groves et al. 1998). As the fluids moved upwards along the shear zones, they experienced P–T changes, altered the host rocks, and deposited their metals and gangue minerals preferentially in dilation zones (Fig. 14). Despite the lack of fluid inclusion data, the Sapucaia, Tucumã and Inajá deposits (Fig. 8) are included in the orogenic gold deposit type, because they display many features consistent with such. The high salinities of the Cumaru ore fluids may reflect an added contribution from a granodiorite magma.

An important issue concerning the Águas Claras deposit refers to the source of the mineralizing fluids that

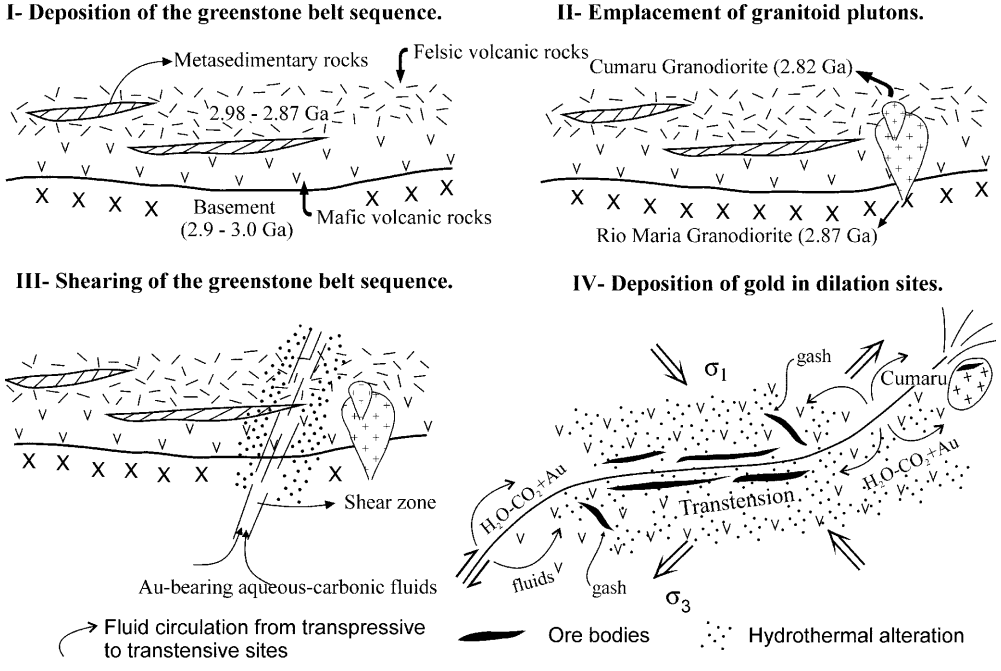

Fig. 14 Model for formation of gold deposits in the Rio Maria granitoid–greenstone terrains, showing the Y-Riedel faults and tension gash vein deposits, as well as the Cumaru granitoid–hosted deposit

were channelled along the shear zone hosting the sulfide- and gold-bearing quartz vein. The short distance (≈5 km) to the granite, and the occurrence of W-, Sn- and F-rich minerals in veins/veinlets, and the highly saline aqueous fluids, strongly support the role of the Serra dos Carajás granite in formation of the Águas Claras mineralization of the ISB. In addition, available isotopic data from the sulfide ores (Table 4) indicate a 2,358 ± 42 Ma age and a 1,880-Ma overprint, with the later coincident with the age of the Serra dos Carajás intrusion. A plausible explanation for the two ages could be the migration of magmatic fluids through pre-existing sulfide accumulations, such as those commonly associated with the Itacaiunas Supergroup units. The magmatic fluids dissolved sulfide minerals and gold and re-precipitated these in favourable sites along the shear zone. Geochemical studies, however, carried out on the Serra dos Carajás granite point to its non-specialized character, making it difficult to be the source for anomalous tin or tungsten in the Águas Claras ore (Barros et al. 1994b; Rios et al. 1995).

Sediment-hosted Au–PGE deposits

In the Serra Pelada deposit, contact relations show that the carbonate and pelitic sequences are concordant, with no stratigraphic disconformity separating them. Furthermore, clasts of banded iron-formation and quartzite in both sequences indicate that they belong to the same sedimentary cycle.

The ilmenite-bearing diorite, which intruded the carbonate sequence, produced a distinct contact aureole. Skarn-like assemblages were formed at temperatures above 550 °C, including diopside and widespread calcite + actinolite (Tallarico et al. 2000a). The thermal effects were much less intense adjacent to intrusions in the pelitic rock sequence in which only white mica (muscovite) is recognized as a characteristic metamorphic phase.

Temporal relationships between the diorite intrusions and the Au–PGE mineralization are still obscure and data are limited, but Tallarico et al. (2000a) suggest that the ore deposition was associated with the hydrothermal system developed surrounding the cooling intrusions. Regardless of their origin, the ore fluids interacted with both the dolomitic marble and intrusions resulting in the precipitation of disseminated sulfide minerals (Tallarico et al. 2000a). They also migrated into highly fractured zones, altering the low-grade metamorphic host rocks and depositing gold and PGE minerals in the carbon-bearing metasiltstones. An important alteration product is the jasperoid layer that marks the contact between the marble and the metasiltstones. This fine-grained, silica-rich rock, despite extending laterally for about 1,200 m, is interpreted to have hydrothermally replaced the dolomitic marble and contains trace amounts of sericite, tourmaline, chlorite, chalcopyrite, hematite and carbonate minerals (Tallarico et al. 2000a). A lithological association analogous with that of the Serra Pelada deposit has been described in the Yankee basin Carlin-type gold orebodies, Nevada, where the contact between the overlying shale and the underlying limestone is marked by a stratiform jasperoid (Hulen and Collister 1999).

The mode of occurrence of the jasperoid layer in Serra Pelada suggests that the ore fluids were impounded at the base of the impermeable grey metasiltstones. Assuming a sulfide-poor hydrothermal system for the Serra Pelada deposit, chloride complexes could have been major gold-transporting agents, but their effectiveness as gold carriers would have required temperatures higher than 450°C (Gammons and Williams-Jones 1997). These temperatures are compatible with those of the initial alteration stage (Tallarico et al. 2000a). Reactions with the carbonate rocks led to fluids becoming progressively alkaline, and favouring gold and PGE precipitation especially as fluids interacted with the carbonaceous units. Estimated temperatures for the ores and associated sulfide minerals are in the 360–230°C range (Tallarico et al. 2000a). The most probable source for the precious metals was the diorites. However, some gold and PGE may have also been leached from the mafic and ultramafic volcanic rocks of the underlying Archean metavolcano-sedimentary sequences. The relatively high contents of cobalt, nickel and palladium in the ore and dark metasiltstones (Meireles and Silva 1988; Tallarico et al. 2000a) corroborate this assumption. Recent geochemical studies indicate that, provided suitable sources are available, both gold and PGE can be scavenged and transported by very acidic oxidized solutions (Wood et al. 1989; Gammons and Williams-Jones 1997).

Hydrothermal fluid circulation during the tectonic event that deformed the metasedimentary rock sequence accounts for the preferential concentration of ore minerals in several structural traps, particularly the fold hinges. A possible evolution of the Serra Pelada deposit is shown in Fig. 15. Later weathering processes caused an exceptional gold enrichment in the supergene profile, generating a residual deposit that is now practically exhausted.

Summary and conclusions

The geological framework of the CMP, largely characterized by Archean metavolcano-sedimentary belts within granitoid–gneissic complexes, was highly favourable for both the introduction of significant amounts of gold and other metals and their concentrations in mineral deposits, albeit not always of economic value.

An attempt is made to provide a provisional classification of the Carajás hypogene gold deposits. In spite of the controversial points concerning their genesis and preliminary nature of much geological data, it is possible to recognize (1) Fe-oxide-poor Cu–Au, (2) Fe-oxide–Cu–Au–U–REE, (3) shear-zone related lode-gold and (4) sedimentary rock-hosted gold-PGE types. Deposits of the first type and some of the second type (Igarapé Salobo and Igarapé Bahia) are interpreted to be synge-

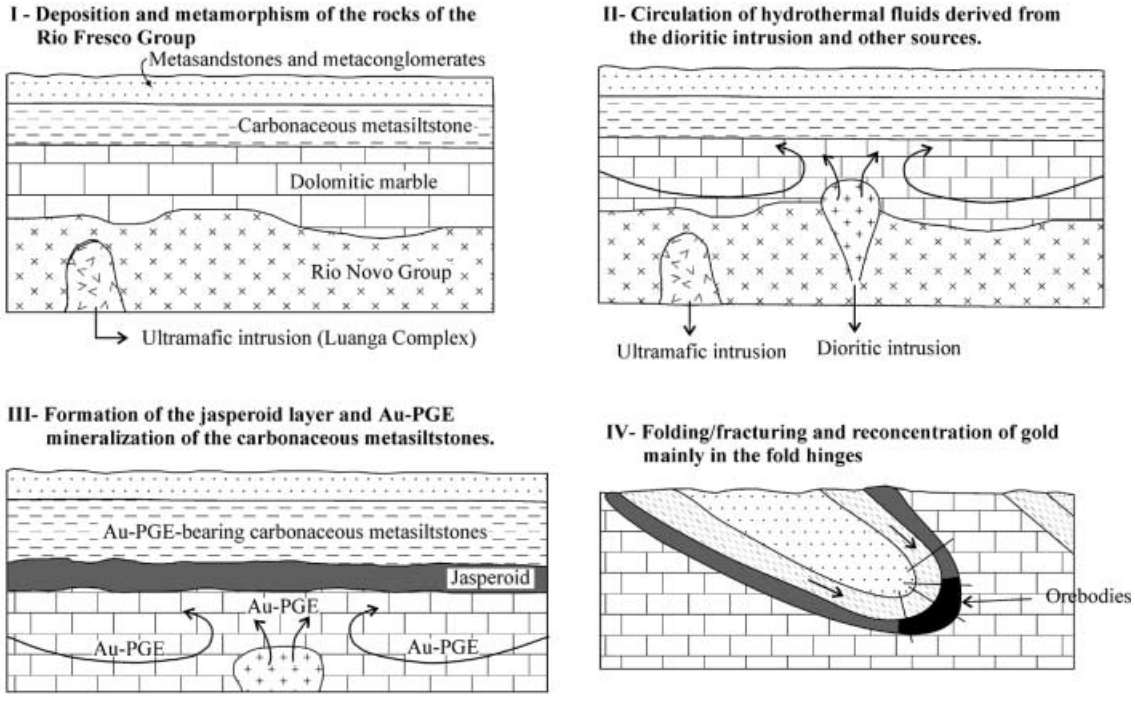

Fig. 15 Genetic model for the Serra Pelada Au–PGE mineralization

netic, of Archean age, and formed in a volcanogenic environment with most metals supplied by magmatic hydrothermal sources. In this sense, they can be broadly envisaged as part of a volcano-plutono-sedimentary system within which ascending magmatic aqueous solutions mixed with seawater and precipitated ores at essentially the same time as the host sequence accumulated. Other deposits of type II (Cristalino and Sossego) are epigenetic and show genetic similarities to those of the Olympic Dam class.

Recycling of those old terrains and successive episodes of shearing, concomitant or not with granitic plutonism, were critical to redistribution of and for the addition of more gold into CMP, leading to metal (re)concentration in a variety of deposits, particularly in auriferous quartz veins along shear zones. Economically, however, it is the magnetite–Cu–Au deposits and Au–PGE deposits in folds that appear most important. Recent weathering processes also were a very effective mechanism for concentrating gold in residual deposits, some of exceptional economic significance.

It is symptomatic that, as recorded in the major Archean cratons worldwide, the Carajás orogenic gold deposits occur preferentially in the RMGGT, where regional shear zones probably represent collisional sutures of crustal blocks and affected the geometry of the greenstone belts themselves. On the other hand, the Fe-oxide-poor Cu–Au and the Fe-oxide–Cu–Au–U–REE types are restricted to the ISB, being related to ensialic extensional basins. The copper–gold shear-zone hosted (Águas Claras) and the sediment-hosted Au–PGE (Serra Pelada) deposits also occur in the ISB, but both were developed in structures produced under an oblique tectonic regime. Significantly, no Cu–Au deposit has yet been discovered in the CMP that is associated with granitic intrusions, but is not hosted by metavolcano-sedimentary sequences. The Sossego deposit, not described in this paper, and the Cristalino deposits are examples of Fe-oxide–Cu–Au–U–REE mineralization hosted in both granitoids and breccias within the metavolcano-sedimentary sequences (Huhn et al. 1999b; Lancaster Oliveira et al. 2000). The Cumaru deposit could represent a typical orogenic gold deposit, but alternatively it may be more like an intrusion-related gold deposit.

The proposed classification is a first effort to work on the systematics of the Carajás gold deposits and hopefully it can be used to develop exploration guidelines in other propitious areas. Despite the gold potential of the Carajás region, very few mines have been opened. At present, only the Igarapé Bahia and Águas Claras mines are in operation, but gold is extracted exclusively from secondary ore.

Acknowledgements On accepting the challenge of writing this paper, the participation of Docegeo geologists was a mandatory condition. Regrettably, this cooperation was restricted to informal talks. Without such indirect cooperation, this paper would have been very difficult to produce. Our acknowledgements are due to all these colleagues. Thanks are also due to Bernd Lehmann (Technical University of Clausthal), David Groves (University of Western Australia), Richard Goldfarb (USGS) and Robert Foster (University of Southampton) for their helpful, insightful and critical comments on earlier versions of this paper.

References

Adshead-Bell NS (1998) Evolution of the Starra and Selwyn high-strain zones, Eastern Fold Belt, Mount Isa inlier: implications for Au–Cu mineralization. Econ Geol 93:1450–1462

Almada MCO (1998) O Corpo Acampamento Sul do depósito Bahia, Carajás: características geológicas e fluidos hidrotermais. MSc Thesis, Universidade Federal do Pará, Centro de Geociências

Almada MCO, Villas RN (1999) O depósito Bahia: um possível exemplo de depósito vulcanogênico tipo Besshi arqueano em Carajás. Rev Bras Geociênc 29:579–592

Almeida FFM (1978) A evolução dos Crátons Amazônico e do São Francisco comparada com seus homólogos do hemisfério norte. In: Cong Bras Geol 30, Proceedings, SBG, Recife, vol 6, pp 2392–2407

Althoff AMR, Villas RN, Giuliani G (1994) A mineralização cuprífera da área Bahia, Serra dos Carajás (PA): evolução dos fluidos hidrotermais e modelo metalogenético. Geoch Brasiliensis 8:135–155

Althoff FJ, Barbey P, Boullier A, Dall'Agnol R (1995) Composição e estrutura dos granitóides arqueanos da região de Marajoara. Bol Museu Paraense Emílio Goeldi (Sér CiêncTerra) 7:5–26

Amaral G (1974) Geologia Pré-cambriana da região Amazônica. Tese de livre docência. São Paulo, Instituto de Geociências, USP

Amaral G (1984) Província Tapajós e Rio Branco. In: Almeida FMA, Hasui Y (ed) O Pré-cambriano do Brasil. Edgard Blücher Ltda, São Paulo, pp 6–35

Amaral EV, Farias NF, Saueressig R, Viana A Jr, Andrade VLL (1988) Jazida de Cobre Salobo 3A e 4A, Serra dos Carajás, Pará, vol 3. In: Schobenhaus C, Coelho CES (co-ord) Principais Depósitos Minerais do Brasil, DNPM, Brasília, pp 43–54

Araújo OJB, Maia RGN, João XSJ, Costa JBS (1988) A megaestruturação arqueana da folha Carajás. In: Simp Latino Americano Geol 7, Belém, SBG. Proceedings, vol 1, pp 324–333

Avelar VG, Lafon JM, Correia FC Jr, Macambira EMB (1999) O magmatismo arqueano da região de Tucumã, Província Mineral de Carajás, Amazônia Oriental, Brasil: novos dados geocronológicos. Rev Bras Geociênc 29:453–460

Barreira CF, Soares ADV, Ronzê PC (1999) Descoberta do depósito Cu-Au Alemão – Província Mineral de Carajás (PA). In: Simp Geol Amaz 6. Expanded Abstr Bull, Manaus, SBG, pp 136–139

Barros CEM (1997) Pétrologie et structure du Complexe Granitique Estrela (2.5 Ga) et son encaissant métavolcano-sédimentaire (Province Metallifère de Carajás, Brésil). PhD Thesis, Université Henri Poncaré, Nancy

Barros CEM, Dall'Agnol R, Lafon JM, Teixeira NP, Ribeiro JW (1992) Geologia e geocronologia Rb–Sr do Gnaisse Estrela, Curionópolis, PA. Bol Museu Paraense Emílio Goeldi (Sér Ciênc Terra) 4:83–102

Barros CEM, Dall'Agnol R, Soares ADV, Dias GS (1994a) Metagabros de Águas Claras, Serra dos Carajás: petrografia, geoquímica e transformações metamórfico-hidrotermais. Acta Geol Leopoldensia 40:31–70

Barros CEM, Dall'Agnol R, Vieira EAP, Magalhães MS (1994b) Granito Serra dos Carajás: uma discussão sobre o seu potencial metalogenético para estanho com base em estudos na borda oeste do corpo. In: Simp Geol Amaz 4, Extended abstr Bull, SBG, Belém, pp 307–309

Beisiegel VR, Bernadelli AL, Drumond NF, Ruff AW, Tremaine JW (1973) Geologia e recursos minerais da Serra dos Carajás. Rev Bras Geociênc 3:215–242

Bell K (1989) Carbonatites, genesis and evolution. Unwin Hyman, London

Chang YA, Goldberg D, Neumann JP (1977) Phase diagrams and thermodynamic properties of ternary copper–silver systems. J Phys Chem Ref Data 6:621–674

Cook NJ, Halls C, Boyle AP (1993) Deformation and metamorphism of massive sulphides at Sulitjelam, Norway. Mineral Mag 57:67–81

Cordani UG, Brito Neves BB (1982) The geologic evolution of South America during the Archaean and Early Proterozoic. Rev Bras Geociênc 12:78–88

Cordani UG, Tassinari CCG, Teixeira W, Basei MAS, Kawashita K (1979) Evolução tectônica da Amazônia com base nos dados geocronológicos. In: Cong Geol Chileno 2, Actas, Santiago, vol 4, pp 137–148

Cordani UG, Tassinari CCG, Kawashita K (1984) A Serra dos Carajás como região limítrofe entre províncias tectônicas. Ciências Terra 9:6–11

Costa JBS, Araujo OJB, Santos A, João XSJ, Macambira MJB, Lafon M (1995) A Província Mineral de Carajás: aspectos tectono-estruturais, estratigráficos e geocronológicos. Bol Museu Paraense Emílio Goeldi (Sér Ciênc Terra) 7:199–235

Costi HT, Dall'Agnol R, Moura CAV (2000) Geology and Pb–Pb geochronology of Paleoproterozoic volcanic and granitic rocks of Pitinga Province, Amazonian Craton, northern Brazil. Int Geol Rev 42:832–849

Craig JR, Vokes FM (1993) The metamorphism of pyrite and pyritic ores: an overview. Mineral Mag 57:3–18

Cunha BCC, Potiguar LAT, Ianhez AC, Bezerra PEL, Pitthan JHL, Souza AMS, Hildred PR, Tassinari CCB (1981) Geologia. In: MME, Projeto Radambrasil, Folha SC-22, Tocantins. Levantamentos de Recursos Naturais. Rio de Janeiro, Convênio DNPM/CPRM/PROPESC, vol 22, pp 21–196

Cunha BCC, Santos DB, Prado P (1984) Contribuição ao estudo da estratigrafia da região de Gradaús, com ênfase no Grupo Rio Fresco. In: Cong Bras Geol 33. Anais, Rio de Janeiro, SBG, vol 2, pp 873–885

Dall'Agnol R, Schuckmann WK, Basei MAS, Scheller T (1984) Novos dados geocronológicos e estudos de elementos traços de maciços graníticos anorogênicos da Amazônia Oriental, Estado do Pará (Brasil). In: Simp Geol Amaz 2, Proceedings, Manaus, MME-DNPM, pp 59–74

Dall'Agnol R, Lafon JM, Macambira MJB (1994) Proterozoic anorogenic magmatism in the Central Amazonian Province, Amazonian Craton: geochronological, petrological and geochemical aspects. Mineral Petrol 50:113–138

Davidson GJ (1992) Hydrothermal geochemistry and ore genesis of sea-floor volcanogenic copper-bearing oxide ores. Econ Geol 87:889–912

Dias GS, Macambira MJB, Dall'Agnol R, Soares ADV, Barros CEM (1996) Datação de zircões de sill de metagabro: comprovação da idade arqueana da Formação Águas Claras, Carajás, Pará. In: Simp Geol Amaz 5, Bull Extended Abstracts, Belém, SBG, pp 376–379

Diella V, Ferrario A, Girardi VAV (1995) PGE and PGM in the Luanga mafic–ultramafic intrusion in Serra dos Carajás (Para State, Brazil). Ore Geol Rev 9:445–453

Docegeo (1988) Revisão litoestratigráfica da Província Mineral de Carajás, Pará. In: Cong Bras Geol 35. Appended to the Proceedings, Belém, SBG, pp 11–54

Duarte KD, Pereira ED, Dall'Agnol R, Lafon JM ((1991) Geologia e geocronologia do granito Mata Surrão – sudeste de Rio Maria (PA). In: Simp Geol Amaz 3, Proceedings, Belém, SBG, pp 7–20

Faraco MTL, Carvalho JMA, Klein EL (1996) Carta metalogenética da Província Carajás – SE do Estado do Pará, Folha Araguaia (SB-22). Nota Explicativa. Belém, CPRM

Farias ES, Villas RN (1996) Rochas ígneas ricas em magnetita, apatita e titanita, Alvo Borrachudo, Carajás (PA). In: Congr Bras Geol 39, Proceedings, SBG, Salvador, vol 3, pp 233–235

Ferreira Filho CF (1985) Geologia e mineralizações sulfetadas do Prospecto Bahia, Província Mineral de Carajás. MSc Thesis, Instituto de Geociências, Universidade de Brasília

Gammons CH, Williams-Jones AE (1997) Chemical mobility of gold in the porphyry–epithermal environment. Econ Geol 92:45–59

Gastal MCP, Macambira MJB, Medeiros H, Dall'Agnol R (1987) Idades e geoquímica isotópica Rb–Sr do granito Musa e do granodiorito Rio Maria, Amazônia Oriental. Geoch Brasil 1:247–259

Gibbs AK, Wirth KR, Hirata WK, Olszewski WJ (1986) Age and composition of the Grão Pará Group volcanics, Serra dos Carajás. Rev Bras Geociênc 16:201–211

Gonçalez MGB, Dall'Agnol R, Vieira EAP, Macambira MJB, Della Senta N (1988) Geologia do maciço anorogênico Cigano,

Vale do Parauapebas (PA). In: Cong Bras Geol 35, Proceedings, SBG, Belém, vol 3, pp 1132–1146
Grguric B, Putnis A (1998) Compositional controls on phase-transition temperatures in bornite: a differential scanning calorimetry story. Can Mineral 36:215–227
Groves DI (1993) The crustal continuum model for late-Archean lode-gold deposits of the Yilgarn Block, Western Australia. Miner Deposita 28:366–374
Groves DI, Foster RP (1991) Archaean lode gold deposits. In: Foster RP (ed) Gold metallogeny and exploration. Blackie, Glasgow, pp 63–103
Groves DI, Goldfarb RJ, Gebre-Mariam M, Hagemann SG, Robert F (1998) Orogenic gold deposits: a proposed classification in the context of their crustal distribution and relationship to other gold deposit types. Ore Geol Rev 13:7–27
Hannington MD, Poulsen KH, Thompson JFH, Sillitoe RH (1999) Volcanogenic gold in the massive sulfide environment. In: Barrie CT, Hannington MD (ed) Volcanic-associated massive sulfide deposits: processes and examples in modern and ancient settings. Rev Econ Geol 8:325–356
Hasui Y, Almeida FFM (1985) The Central Brazil Shield reviewed. Episodes 8:29–37
Hasui Y, Haralyi NLE, Costa JBS (1993) Megaestruturação pré-cambriana do território brasileiro baseada em dados geofísicos e geológicos. Geociências 12:7–31
Herzig PM, Hannington MD, Fouquet Y, von Stalckelberg U, Petersen S (1993) Gold-rich polymetallic sulfides from the Lau Back Arc and implications for the geochemistry of gold in sea-floor hydrothermal systems of the Southwest Pacific. Econ Geol 88:2182–2209
Hirata WK, Rigon JC, Kadekaru K, Cordeiro AAC, Meireles EM (1982) Geologia regional da Província Mineral de Carajás. In: Simp Geol Amaz 1, Proceedings, Belém, SBG, pp 100–110
Hitzman MW, Oreskes N, Einaudi MT (1992) Geological characteristics and tectonic setting of Proterozoic iron oxide (Cu–Au–U–REE) deposits. Precambrian Res 58:241–287
Huhn SRB, Nascimento JAS (1997) São os depósitos cupríferos de Carajás do tipo Cu–Au–U–ETR? In: Costa ML, Angélica RS (co-ord) Contribuições à Geologia da Amazônia, FINEP-SBG, pp 143–160
Huhn SRB, Santos ABS, Amaral AF, Ledshan EJ, Gouvea JL, Martins LPB, Montalvão RGM, Costa VG (1988) O terreno 'granito greenstone' da Região de Rio Maria, sul do Pará. In: Cong Bras Geol 35, Anais, Belém, SBG, vol 3, pp 1438–1452
Huhn SRB, Macambira MJB, Dall'Agnol R (1999a) Geologia e geocronologia Pb–Pb do granito alcalino arqueano Planalto, região da Serra do Rabo, Carajás, PA. In: Simp Geol Amaz 5, Bull Extended Abstr, Manaus, SBG, pp 463–466
Huhn SRB, Souza CIJ, Albuquerque MC, Leal ED, Brustolin V (1999b) Descoberta do depósito Cu(Au) Cristalino: geologia e mineralização associada, região da Serra do Rabo, Carajás-PA. In: Simp Geol Amaz 5, Bull Extended abstr, Manaus, SBG, pp 140–143
Huhn SRB, Soares ADV, Souza CIJ, Albuquerque MAC, Leal ED, Vieira EAP, Masotti FS, Brustolin V (2000) The Cristalino copper–gold deposit, Serra dos Carajás, Pará. In: Intern Geol Congress 31, Abstr vol (CD-Rom), Rio de Janeiro, IUGS
Hulen JB, Collister JW (1999) The oil-bearing, Carlin-type gold deposits of Yankee basin, Alligator Ridge District, Nevada. Econ Geol 94:1029–1050
Humphris SE, Thompson G (1978) Hydrothermal alteration of oceanic basalts by seawater. Geochim Cosmochim Acta 42:107–125
Kerswill JA (1993) Models for iron-formation-hosted gold deposits. In: Kirkham RV, Sinclair WD, Thorpe RI, Duke JM (ed) Mineral deposit modeling, Geol Soc Can, Spec Pap 40:171–199
Knup PE (1971) Reconhecimento geológico da região dos rios Itacaiúnas e Tocantins, estado do Pará. In: Cong Bras Geol 25, Abstr, SBG, São Paulo, pp 61–62
Lafon JM, Sheller T (1994) Geocronologia Pb–Pb em zircão do granodiorito Cumaru, Serra dos Carajás, Pará. In: Simp Geol Amaz 4, Bull Extended Abstr, Belém, SBG, pp 321–324
Lafon JM, Macambira MJB, Scheller T, Garcia R (1988) Relatório sobre o estudo geocronológico Rb–Sr do maciço granítico da Serra da Seringa e dos granulitos da Serra do Pium (PA), Conv FADESP/CPRM-Belém. unpublished final report
Lafon JM, Pereira ED, Macambira EMB, Vale AG, Barradas JAS (1991) Geocronologia Rb–Sr da região de São Félix do Xingu: resultados preliminares. In: Simp Geol Amaz 3, Proceedings, SBG, Belém, pp 21–35
Lancaster Oliveira J, Fanton J, Almeida AJ, Leveille RA, Vieira S (2000) Discovery and geology of the Sossego copper–gold deposit, Carajás District, Pará State, Brazil. In: Intern Geol Congr 31, Abstracts vol (CD-Rom), Rio de Janeiro, IUGS
Lindenmayer ZG (1990) Salobo Sequence, Carajás, Brazil: geology, geochemistry and metamorphism. PhD Thesis, University of Western Ontario
Lindenmayer ZG, Bocalon VLS (1997) Caracterização da mineralização primária da mina de Au do Igarapé Bahia, Serra dos Carajás. In: Marini OJ (ed) Caracterização de minérios e rejeitos de depósitos minerais brasileiros – estudos texturais, química mineral e varredura química. DNPM-PADCT, pp 17–20
Lindenmayer ZG, Fyfe WS (1994) The Salobo Cu (Au, Ag, Mo) deposit, Serra dos Carajás, Brazil. In: Congr Geol Chileno 7. Concepción, Atas vol 2, pp 840–842
Lindenmayer ZG, Teixeira JBG (1999) Ore genesis at the Salobo copper deposit, Serra dos Carajás. In: Silva MG, Misi A (ed) Base metal deposits of Brazil MME/CPRM/DNPM, Belo Horizonte, pp 33–43
Macambira MJB (1992) Chronologie U–Pb, Rb–Sr, K–Ar et croissance de la croûte continental dans l'Amazonie du sud-est: example de la région de Rio Maria, Province de Carajás, Brésil. PhD Thesis, Université de Montpellier II
Macambira MJB, Lancelot J (1996) Time constraints of the Archean Rio Maria crust, Southeastern Amazonian Craton, Brazil. Int Geol Rev 38:1134–1142
Macambira MJB, Lafon JM, Barradas JA (1991) Le granite Xinguara, témoin d'un magmatisme monzogranitique dans l'archéen de l'Amazonie orientale, Brésil. C R Acad Sci Paris 313(II):781–785
Machado N, Lindenmayer Z, Krogh TE, Lindenmayer D (1991) U–Pb geochronology of Archean magmatism and basement reactivation in the Carajás area, Amazon shield, Brasil. Precambrian Res 49:329–354
Medeiros Neto FA, Villas RN (1985) Geologia da jazida de Cu-Zn do Corpo 4E-Pojuca, Serra dos Carajás. In: Simp Geol Amaz 2, Proceedings, SBG, Belém, vol 3, pp 97–112
Meireles EM, Silva ARB (1988) Depósito de ouro de Serra Pelada, Marabá, Pará. In: Schobbenhaus C, Coelho CES (co-ord) Principais depósitos minerais brasileiros (metais básicos não ferrosos, ouro e alumínio), DNPM-CVRD, vol 3, pp 547–558
Meireles EM, Teixeira JT, Medeiros Filho CA (1982) Geologia preliminar do depósito de ouro de Serra Pelada. In: Simp Geol Amaz 1, Proceedings, SBG, Belém, vol 2, pp 74–84
Mellito KM, Tassinari CCG (1998) Aplicação dos métodos Rb–Sr e Pb–Pb à evolução da mineralização cuprífera do depósito de Salobo 3 α, Província Mineral de Carajás, Pará. In: Cong Bras Geol 40, Proceedings, Belo Horizonte, SBG, p 119
Mottl MJ (1983) Metabasalts, axial hot springs, and the structure of hydrothermal systems at mid-ocean ridge. Bull Geol Soc Am 94:161–180
Mougeot R, Respaut JP, Briqueu L, Ledru P, Milesi JP, Lerouge C, Marcoux E, Huhn SB, Macambira MJB (1996) Isotope geochemistry constraints for Cu, Au mineralizations and evolution of the Carajás Province (Pará, Brazil). In: Cong Bras Geol 39, Extended Abstr Bull, SBG, Salvador, vol 7, pp 321–324
Moura CAV, Gaudette HE (1993) Evidence of Brasiliano/Panafrican deformation in the Araguaia belt: implication for Goldwana evolution. Rev Bras Geociênc 23:117–123
Nogueira ACR (1995) Análise faciológica e aspectos estruturais da Formação Águas Claras, região central da Serra dos Carajás. MSc Thesis, Centro de Geociências, Universidade Federal do Pará

Nogueira ACR, Truckenbrodt W, Pinheiro RLV (1995) Formação Águas Claras, Pré-cambriano da Serra dos Carajás: redescrição e redefinição litoestratigráfica. Bol Museu Paraense Emílio Goeldi (Sér Ciênc Terra) 7:177–197

Oliveira CG, Leonardos OH (1990) Gold mineralization in the Diadema shear belt, Northern Brazil. Econ Geol 85:1034–1043

Oliveira CG, Santos RV, Leonardos OH (1995) Geologia e mineralização aurífera do greenstone belt Sapucaia, Sudeste do Pará. Bol Museu Paraense Emílio Goeldi (Sér Ciênc Terra) 7:61–91

Oliveira CG, Tavaza E, Tallarico F, Santos RV, Gomes C (1998) Gênese do depósito de Au–Cu–(U–ETR) do Igarapé Bahia, Província Mineral de Carajás. In: Cong Bras Geol 40, Proceedings, SBG, Belo Horizonte, p 137

Oreskes N, Einaudi M (1990) Origin of rare-earth element-enriched hematite breccias at the Olympic Dam Cu–U–Au–Ag deposit, Roxby Downs, South Australia. Econ Geol 85:1–29

Oreskes N, Hitzman MW (1993) A model for the origin of Olympic Dam-type deposits. In: Kirkham RV, Sinclair WD, Thorpe RI, Duke JM (ed) Mineral deposit modeling. Geol Soc Can, Spec Pap 40:615–634

Pereira ED (1992) Contribuição à evolução geológica da parte oriental da Província Amazônia Central através da geocronologia Rb–Sr da Província Mineral de Carajás e região de São Félix do Xingu, PA. MSc Thesis, Centro de Geociências, Universidade Federal do Pará

Pidgeon RT, Macambira MJB (1998) Datação U–Pb de estruturas primárias e secundárias de zircões de granulitos do Complexo Pium, Província Carajás, Pará. In: Congr Bras 40, Proceedings, Belo Horizonte, SBG, p 56

Pimentel MM, Machado N (1994) Geocronologia U–Pb dos terrenos granito–greenstone de Rio Maria, Pará. In: Congr Bras Geol 38, Proceedings, SBG, Camboriu, vol 2, pp 390–391

Pinheiro RVL (1997) Reactivation history of the Carajás and Cinzento strike-slip systems, Amazon, Brazil. PhD Thesis, Department of Geological Sciences, University of Durham

Pinheiro RVL, Holdsworth RE (1997) Reactivation of Archean strike-slip fault systems, Amazon region, Brazil. J Geol Soc Lond 154:99–103

Poulsen KH, Card K, Mortensen J, Robert F (1992) Plate tectonics and the mineral wealth of the Canadian Shield. Geotimes 37(8):19–21

Reis FN (2000) Origem e evolução do depósito de sulfetos de Serra Verde, Curionópolis (PA), com base em dados geológicos, petrográficos, mineralógicos e isotópicos de Pb. MSc Thesis, Centro de Geociências, Universidade Federal do Pará

Reis FN, Villas RN (1999) O depósito de sulfetos de Cu–Au de Serra Verde, Província Mineral de Carajás: caracterização mineralógica, rochas encaixantes e evidências de metamorfismo. In: Simp Geol Amaz 6, Bull Extended Abstr, SBG, Manaus, pp 106–109

Réquia KCM, Xavier RP, Figueiredo B (1995) Evolução paragenética, textural e das fases fluidas no depósito polimetálico do Salobo, Província Mineral de Carajás, Pará. Bol. Museu Paraense Emílio Goeldi (Série Ciências da Terra) 7:27–39

Rios FJ, Villas RN, Dall'Agnol R (1995) O granito Serra dos Carajás, Pará: I. Fácies petrográficas e avaliação do potencial metalogenético para estanho no setor norte. Rev Bras Geociênc 25:20–31

Roberts RG (1987) Archean lode-gold deposits. Ore Deposits Models no 11, Geosci Can 14:37–52

Rodrigues ES, Lafon JM, Scheller T (1992) Geocronologia Pb–Pb da Província Mineral de Carajás: primeiros resultados. Cong Bras Geol 37, Bull Extended Abstr, SBG, São Paulo, vol 2, pp 183–184

Roth T, Thompson JFH, Barrett TJ (1999) The precious metal-rich Eskay Creek deposit, Northwestern British Columbia. In: Barrie CT, Hannington MD (ed) Volcanic-associated massive sulfide deposits: processes and examples in modern and ancient settings. Rev Econ Geol 8:357–374

Rotherham JF (1997) A metasomatic origin for the iron-oxide–Au–Cu Starra orebodies, Eastern Fold Belt, Mount Isa Inlier. Mineral Deposita 32:205–218

Santos BA (1981) Amazônia – Potencial mineral e perspectivas de desenvolvimento. Editora da Universidade de São Paulo, São Paulo

Santos MD (1995) O papel dos granitóides na gênese dos depósitos de ouro tipo lode arqueano: caso da jazida do Cumaru – PA. PhD Thesis, Instituto de Geociênciências, Universidade de Brasília

Santos MD, Leonardos OH (1995) Sistema de fluidos e modelo genético do depósito aurífero de Cumaru, SE do estado do Pará. Bol Museu Paraense Emílio Goeldi (Sér Ciênc Terra) 7:237–262

Santos MD, Leonardos OH, Foster RP, Fallick AE (1998) The lode-porphyry model as deduced from the Cumaru mesothermal granitoid–hosted gold deposit, Southern Pará, Brazil. Rev Bras Geociênc 28:345–360

Santos JOS, Hartmann LA, Gaudette HE, Groves DI, McNaughton NJ, Fletcher IR (2001) A new understanding of the Provinces of the Amazon Craton based on integration of field mapping and U–Pb and Sm–Nd geochronology. Gondwana Res (in press)

Sato K, Tassinari CCG (1997) Principais eventos de acreção continental no Cráton Amazônico baseados em idade modelo Sm–Nd, calculada em evoluções de estágio único e estágio duplo. In: Costa ML, Angélica RS (eds) Contribuições à geologia da Amazônia. FINEP-SBG, Belém, pp 91–142

Schobbenhaus C, Campos DA (1984) A evolução da Plataforma Sul-americana no Brasil e suas principais concentrações minerais. In: Schobbenhaus C, Campos DA, Derze GR, Asmus HE (ed) Geologia do Brasil: Texto Explicativo do Mapa Geológico do Brasil e da Área Oceânica Adjacente, incluindo Depósitos Minerais. Brasília, DNPM, pp 9–55

Schobbenhaus C, Campos DA, Derze GR, Asmus HE (1981) Mapa geológico do Brasil e da área oceânica adjacente, incluindo os depósitos minerais. Brasília, Ministério das Minas e Energia/DNPM

Silva CMG (1996a) O prospecto Águas Claras, Carajás (PA): alteração hidrotermal e mineralização de sulfetos associada. MSc Thesis, Centro de Geociênciências, Universidade Federal do Pará

Silva CMG, Villas RN (1998) The Águas Claras Cu-sulfides ± Au deposit, Carajás region, Pará, Brazil: geological setting, wall-rock alteration and mineralizing fluids. Rev Bras Geociênc 28:331–334

Silva ERP (1996b) Geologia e geoquímica das mineralizações de ouro das áreas Salobo e Pojuca-Leste, Serra dos Carajás. PhD Thesis, Centro de Geociências, Universidade Fedral do Pará

Silva GG, Lima MIC, Andrade ARF, Issler RS, Guimarães G (1974) Geologia. Folha SB-22 Araguaia e parte SC-22 Tocantins. Projeto Radambrasil, vol 4, pp 2–30 (Levantamento de Recursos Minerais)

Silva RO Jr, Dall'Agnol R, Oliveira EP (1996) Geologia, geoquímica e geocronologia K–Ar dos diques da região de Rio Maria, sudeste do estado do Pará. In: Simp Geol Amaz 5. Bull Expanded Abstr, Belém, SBG, pp 384–387

Siqueira JB, Costa JBS (1991) Evolução geológica do duplex Salobo-Mirim. In: Simp Geol Amaz 3. Proceedings, Belém, pp 232–243

Slack JF (1996) Tourmaline association with hydrothermal ore deposits. In: Grew ES, Anovitz LM (ed) Boron. Mineralogy, petrology and geochemistry. Mineral Soc Am Rev Mineral 33:559–643

Soares ADV, Santos AB, Vieira EA, Bella VM, Martins LPB (1994) Área Águas Claras: contexto geológico e mineralizações. In: Simp Geol Amaz 4, Bull Extended Abstr, Belém, SBG, pp 379–382

Soares ADV, Ronzê PC, Santos MGS, Leal ED, Barreira CF (1999) Geologia e mineralizações do depósito de Cu–Au Alemão, Província Mineral de Carajás (PA). In: Simp Geol Amaz 6. Bull Expanded Abstr, Manaus, SBG, pp 144–147

Souza CS (1999) Gênese e controle do depósito aurífero de Lagoa Seca, greenstone-belt de Andorinhas, Rio Maria – PA. MSc Thesis, Instituto de Geociênciências, Universidade de Brasília

Souza SRB, Macambira MJB, Scheller T (1996) Novos dados geocronológicos para os granitos deformados do rio Itacaiúnas (Serra dos Carajás, Pará): implicações estratigráficas. In: Simp Geol Amaz 5. Bull Expanded abstr, Belém, SBG, pp 380–383

Suita MTF (1988) Geologia da área Luanga com ênfase na petrologia do Complexo máfico–ultramáfico Luanga e depósitos de cromita associados. MSc Thesis, Instituto de Geociências, Universidade de Brasília

Sutec/CVRD (1996) Projeto de revisão do modelo geológico da mina do Igarapé Bahia: petrografia, química mineral e litogeoquímica. Internal report

Tallarico FHB, Rego JL, Oliveira CG (1998) A mineralização de Au–Cu de Igarapé Bahia – Carajás: um depósito da classe óxido de Fe (Cu–U–Au–ETR). In: Congr Bras Geol 40. Proceedings, SBG, Belo Horizonte, p 116

Tallarico FHB, Coimbra CR, Costa CHC (2000a) The Serra Leste sediment-hosted Au-(Pd–Pt) mineralization, Carajás Province. Rev Bras Geociênc 30:226–229

Tallarico FHB, Oliveira CG, Figueiredo BR (2000b) The Igarapé Bahia Cu–Au mineralization, Carajás Province. Rev Bras Geociênc 30:230–233

Tassinari CCG, Macambira MJB (1999) Geochronological provinces of the Amazonian Craton. Episodes 22:174–182

Tazava E (1999) Mineralização de Au–Cu–(±ETR–U) asssociada às brechas hidrotermais do depósito de Igarapé Bahia, Província Mineral de Carajás, PA. MSc Thesis, Escola de Minas, Universidade Federal de Ouro Preto

Teixeira W, Tassinari CCB, Cordani UG, Kawashita K (1989) A review of the geochronology of the Amazonian Craton: tectonic implications. Precambrian Res 42:213–227

Trendall AF (1983) Introduction. In: Trendall AF, Morris RC (ed) Iron-formation: facts and problems. Developments in Precambrian geology, vol 6. Elsevier, Amsterdam, pp 1–12

Trendall AF, Basei MAS, De Laeter JR, Nelson DR (1998) SHRIMP U–Pb constraints on the age of the Carajás formation, Grão Pará Group, Amazon Craton. J S Am Earth Sci 11:265–277

Vieira EAP, Siqueira JB, Silva ERP, Rego JL, Castro FDC (1988) Caracterização geológica da jazida polimetálica do Salobo 3A – Reavaliação. In: Cong Bras Geol 35. Província Mineral de Carajás – Litoestratigrafia e Principais Depósitos Minerais. Anexo aos Anais, Belém, SBG, pp 97–114

Villeneuve ME, Relf C (1998) Tectonic setting of 2.6 Ga carbonatites in the Slave Province, Canada. J Petrol 39:1975–1986

Viveiros JF (1999) Jazida de Serra Leste se limita a 30 toneladas de ouro. O Liberal, Belém, 06.22.99

Winter CJ (1995) Geology and base-metal mineralization associated with Archean iron-formations in the Pojuca Corpo Quatro deposit, Carajás, Brazil. PhD Thesis, University of Southampton

Wirth KR, Gibbs AK, Olszewski WJ Jr (1986) U–Pb ages of zircons from the Grão Pará Group and Serra dos Carajás granite, Pará, Brasil. Rev Bras Geociênc 16:195–200

Wood SA, Mountain BW, Fenlon BJ (1989) Thermodynamic constraints on the solubility of platinum and palladium in hydrothermal solutions: reassessment of hydroxide, bisulfide, and ammonia complexing. Econ Geol 84:2020–2028

Zang W, Fyfe WS (1995) Chloritization of the hydrothermally altered bedrock at the Igarapé Bahia gold deposit, Carajás, Brazil. Mineral Deposita 30:30–38